AFRL-RD-PS
TP-2010-1008

SNR LIMITS TO ACHIEVING THE CRAMER-RAO LOWER BOUNDS WITH PCID

Chuck Matson
Mike Flanagan
Tony Vincent

Air Force Research Laboratory
3500 Aberdeen Ave SE
Kirtland AFB, NM 87117

1 January 2010

Conference Proceeding

AIR FORCE RESEARCH LABORATORY
Directed Energy Directorate
3550 Aberdeen Ave SE
AIR FORCE MATERIEL COMMAND
KIRTLAND AIR FORCE BASE, NM 87117-5776

REPORT DOCUMENTATION PAGE

Form Approved
OMB No. 0704-0188

1. REPORT DATE *(DD-MM-YYYY)*	2. REPORT TYPE	3. DATES COVERED *(From - To)*
01/01/2010	Conference Proceeding	Jan 7, 2007- Jan 1, 2010

4. TITLE AND SUBTITLE

SNR Limits to Achieving the Cramer-Rao Lower Bounds with PCID

5a. CONTRACT NUMBER
In House DF701944

5b. GRANT NUMBER

5c. PROGRAM ELEMENT NUMBER
61102F

6. AUTHOR(S)

Chuck Matson, Mike Flanagan, Tony Vincent

5d. PROJECT NUMBER
2301

5e. TASK NUMBER
S3

5f. WORK UNIT NUMBER
01

7. PERFORMING ORGANIZATION NAME(S) AND ADDRESS(ES)

Air Force Research Laboratory
3500 Aberdeen Ave SE
Kirtland AFB, NM 87117-5776

8. PERFORMING ORGANIZATION REPORT NUMBER

9. SPONSORING / MONITORING AGENCY NAME(S) AND ADDRESS(ES)

10. SPONSOR/MONITOR'S ACRONYM(S)

AFRL/RDSA

11. SPONSOR/MONITOR'S REPORT NUMBER(S)
AFRL-RD-PS-TP-2010-1008

12. DISTRIBUTION / AVAILABILITY STATEMENT

Approved for Public Release

13. SUPPLEMENTARY NOTES

Accepted for presentation at the AFOSR review; Feb 11, 2010; Maui HI. 377ABW-2010-0184; Feb 9, 2010. "Government Purpose Rights"

14. ABSTRACT

We conducted this research to better understand how Cramer-Rao lower bounds can be used to understand the performance of multi-frame blind deconvolution algorithms such used to understand the performance of multi-frame blind deconvolution algorithms such as PCID. It was clear from previous results that we generated that the image-domain sample variances from PCID deviated from the CRBs significantly more than was expected given the signal-to-noise ratios of the data. It was our suspicion that the Fourier domain was a better place to carry out this investigation. It will be shown that this is true.

15. SUBJECT TERMS

16. SECURITY CLASSIFICATION OF:			17. LIMITATION OF ABSTRACT	18. NUMBER OF PAGES	19a. NAME OF RESPONSIBLE PERSON
a. REPORT	b. ABSTRACT	c. THIS PAGE			Chuck Matson
Unclassified	Unclassified	Unclassified	SAR	46	19b. TELEPHONE NUMBER *(include area code)* 505-846-2049

Standard Form 298 (Rev. 8-98)
Prescribed by ANSI Std. 239.18

This page is intentionally left blank.

Outline

- Purpose for the research
- Imaging model
- PCID
- Cramér-Rao lower bound theory
- Results
- Conclusions

This work is funded by the Air Force Office of Scientific Research and the Air Force Research Laboratory

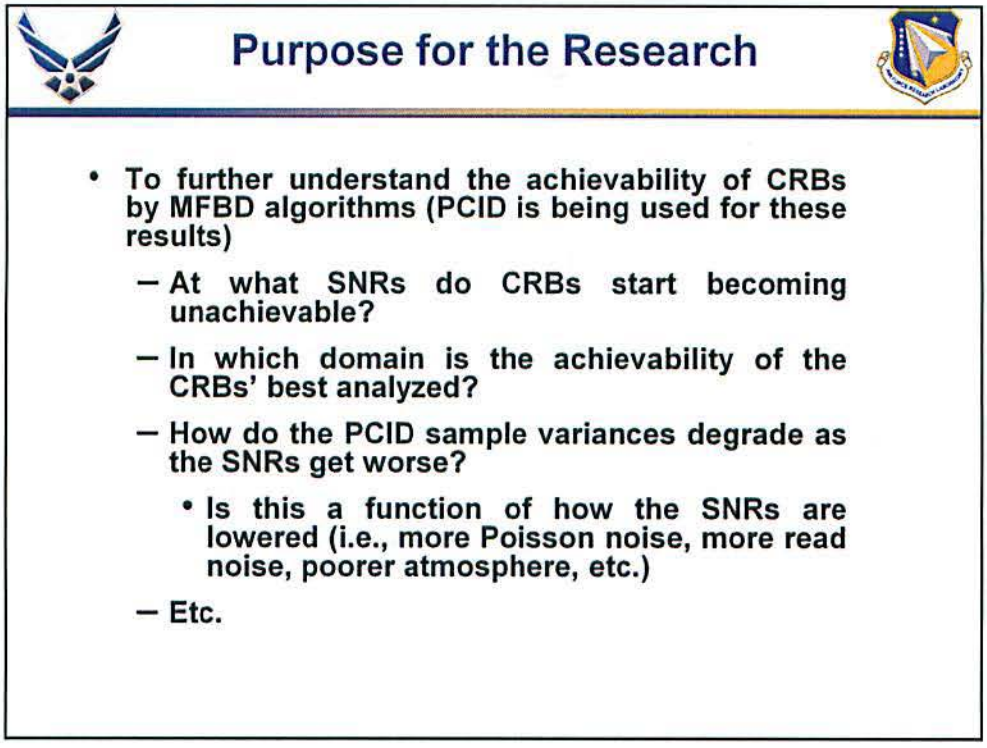

We conducted this research to better understand how Cramer-Rao lower bounds can be used to understand the performance of multi-frame blind deconvolution algorithms such as PCID. It was clear from previous results that we generated that the image-domain sample variances from PCID deviated from the CRBs significantly more than was expected given the signal-to-noise ratios of the data. It was our suspicion that the Fourier domain was a better place to carry out this investigation. It will be shown that this is true.

Imaging Model

- **Raw measurements $\{i_m(x)\}$, m=1,…,M, are modeled as**

$$i_m(\mathbf{x}) = h_m(\mathbf{x}) * o(\mathbf{x}) + n_m(\mathbf{x})$$

where o(x) is the true object, $h_m(x)$ is the point spread function (PSF) blurring the measured data, and $n_m(x)$ is zero-mean noise for the m^{th} image

  - **$n_m(x)$ models both read noise and Poisson noise**
  - **$h_m(x)$ is invertible - derived from atmospheric PSFs**

This is the standard simple linear imaging model. The only difference that we impose is that the PSFs must be invertible. This is necessary to be able to calculate the CRBs. Although this means that we didn't use realistic PSFs, we believe that the conclusions we draw will be extensible to realistic PSFs.

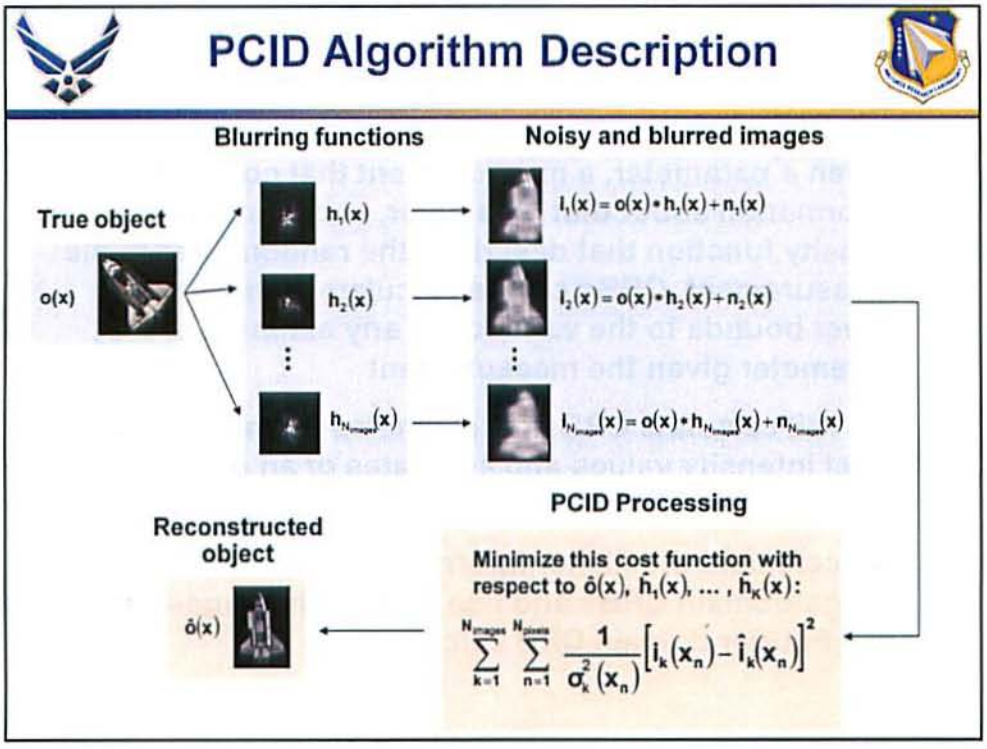

This is a flowchart of the PCID algorithm showing the cost function, the equations describing the measurements, and a sample reconstruction. This chart was taken from a previously-cleared briefing (Case Number RD08-0211)

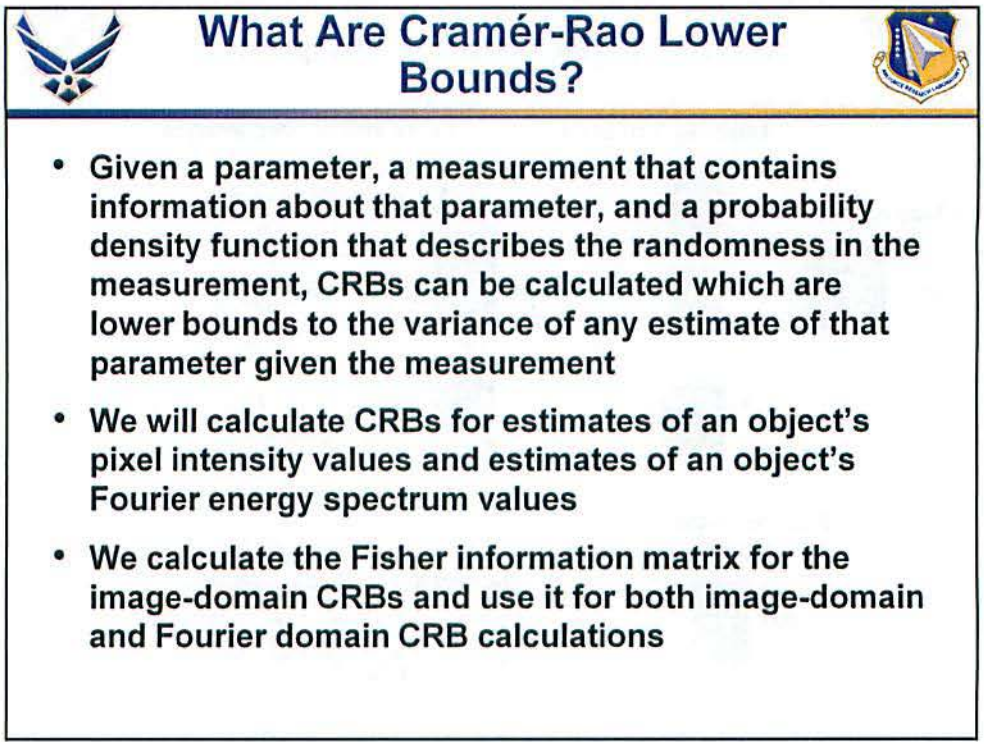

Standard textbook description of Cramer-Rao lower bounds.

Our Previous PCID/CRB Results

Non-blind results

Scenario	PCID/CRB Ratios		
	Mean	Minimum	Maximum
Non-blind and unbiased estimation	0.9904	0.9402	1.0326
Non-blind and Tikhonov-regularized estimation	1.0235	0.9627	1.0768

Blind results

Noise Values	PCID/CRB Ratios	
	OCNR	Two-clrc
Single-pixel read noise variance = 0.1	1.013	1.024
Single-pixel read noise variance = 1.0	1.205	1.172
Single-pixel read noise variance = 2.0	1.321	1.306
Photon noise for 10^9 photons	1.014	0.994
Photon noise for 10^8 photons	1.173	1.181

C. L. Matson, et al."Fast and optimal multi-frame blind deconvolution algorithm for high-resolution ground-based imaging of space objects," *Applied Optics* 48, A75-A92 (2009)

In our previous work, we carried out an extensive number of comparisons between PCID sample variances and the associated CRBs for non-blind deconvolution. As can be seen in the top table, there is close agreement between the two.

For blind results, the story is quite different. We were only able to get five comparisons between PCID and CRBs in time for the paper. We can see that, as the SNRs of the data decrease, the match gets worse. But the match seems to be much worse that would be expected from the absolute values of the data SNRs. The purpose of this presentation is to explore this issue further.

Tables from previously-cleared paper Case Number RD08-0211.

CRBs Can Be Achieved For High-SNR Data

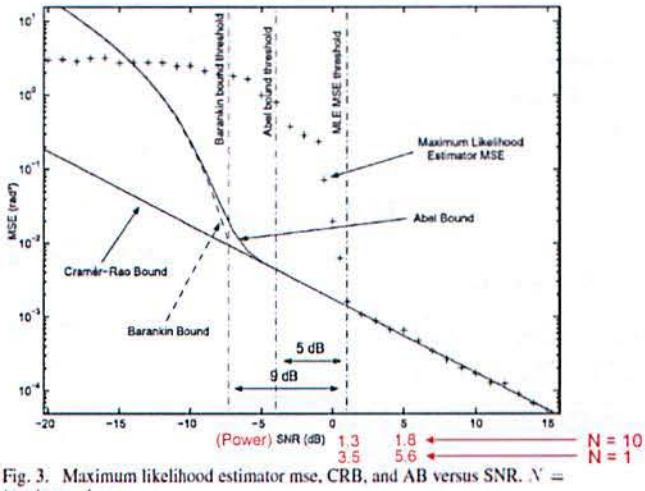

Fig. 3. Maximum likelihood estimator mse, CRB, and AB versus SNR. $N = 10$ observations.

A Useful Form of the Abel Bound and Its Application to Estimator Threshold Prediction
Alexandre Renaux, Leila Najjar-Atallah, Philippe Forster, and Pascal Larzabal
IEEE TRANSACTIONS ON SIGNAL PROCESSING, VOL. 55, NO. 5, MAY 2007, 2365-2369

This figure is from the referenced paper. The important thing to observe in this figure is that the MLE MSEs match the CRBs very well for SNRs > 3.5 or so, and then become much larger than the CRBs. As will be shown, we can't get this kind of curve using image-domain CRBs, but we can in the Fourier domain.

CRB & PCID Calculation Parameters

- Atmospheric PSFs, $D/r_0 = 8$, made invertible, two versions
- Read & Poisson noises
- Support constrained restorations
  - PSF supports: circles – truth, 4x the area of truth
  - Object supports: true and (smallest) circular
- No positivity constraints or regularization used

ocnr psf1 psf2

These are the parameters for the CRB and PCID calculations. The two PSFs used for the results were generated from simulated D/ro = 8 data, but then clipped by circular supports. The radius of PSF2's clipping is twice as large as PSF1's clipping, so PSF2 has four times the area of PSF1.

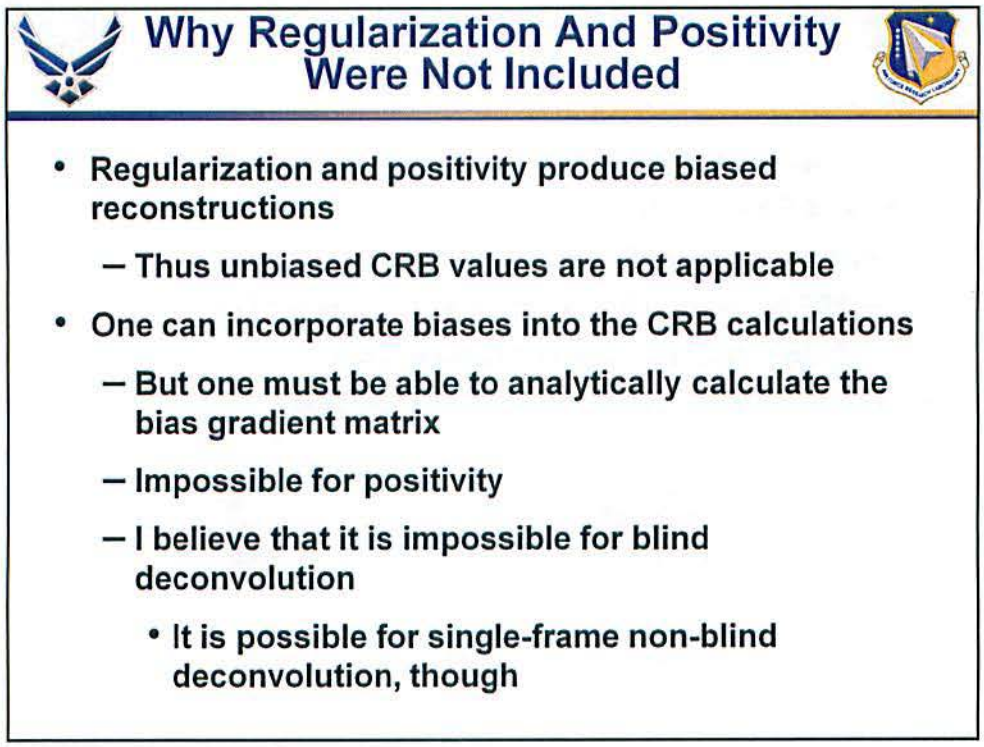

In essence, I don't know how to calculate CRBs for positivity-constrained or regularized MFBD. I'm not sure that there is a way to do so. But since I don't know how, I don't include them in the results.

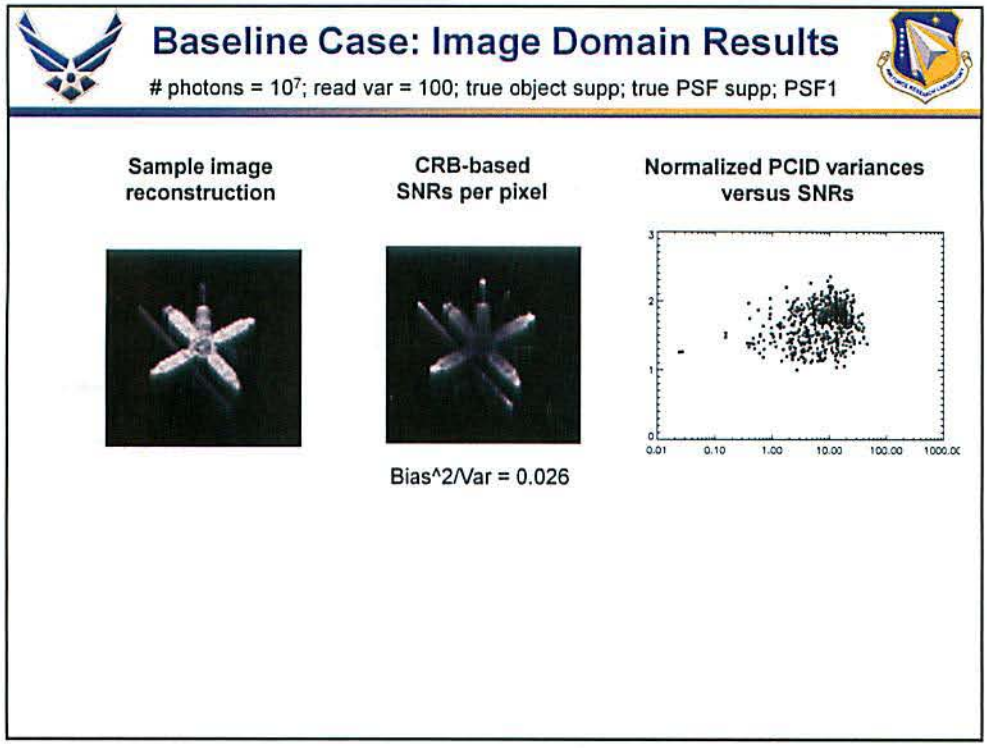

This is the baseline case against which all other results are compared. The CRBs and PCID sample variances describe how accurately PCID was able to reconstruct the true object intensity values per pixel. The parameter values used for the baseline case are shown above, and result in nice-looking reconstructions (left-most figure). The middle figure is the CRB-based image-domain SNRs. It was generated by dividing the true object by the square root of the image-domain CRBs. The right-most figure is a scatterplot. Each point corresponds to a pixel location in the image domain, and each point is the value of the ratio of the PCID sample variance at that pixel location to the CRB at that pixel location. This figure corresponds to the figure on slide 8, where in both figures the horizontal axis is SNR on a log scale. The vertical axis in the figure on slide 8 is mean square error. The vertical axis in this figure is normalized variance. Because we are seeking unbiased estimates, normalized variance is equal to normalized MSE. The term 'normalized' means that the sample PCID variances are divided by the CRBs, so for each pixel, the normalized CRBs are just one. Recall that we want to replicate the shape of the CRB curve and the sample variance curve in the figure on slide 8, where the CRBs and sample variances are equal to each other for high SNRs, and deviate at low SNRs, with the PCID sample variances higher than the CRBs. Notice that this isn't the case. Thus, the image domain is not the right place to carry out this analysis.

Recall that the CRBs being calculated are lower bounds to unbiased estimates of the image intensity values per pixel. We monitor the bias of the PCID reconstructions to see if they are truly unbiased. On all the slides, the image-domain ratio of bias^2 to variance (the appropriate measure) is given. Generally speaking, we consider a PCID reconstruction to be essentially unbiased if this ratio is much less than 0.1.

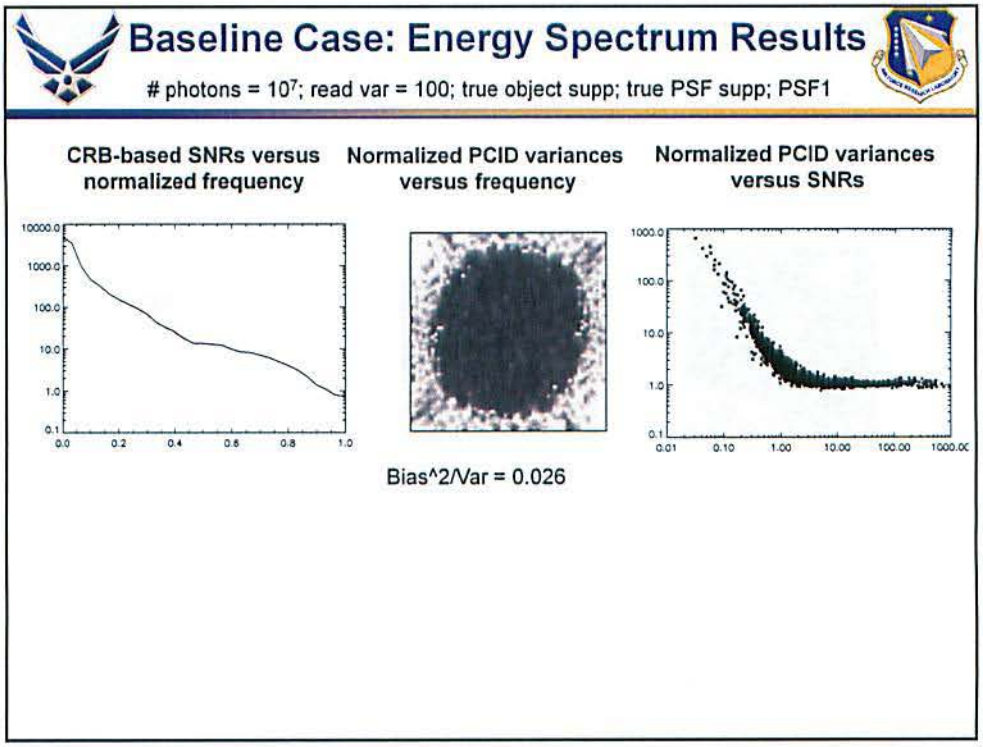

This is the baseline case against which all other results are compared, looked at in the Fourier domain. To generate these results, we calculate the energy spectrum of each PCID reconstruction and calculate sample variances for the energy spectrum estimate. It is important to realize that we don't estimate the energy spectrum directly from the data, as is the case for speckle imaging. We calculate the PCID reconstructions directly, and then transform to the energy spectrum domain.

Similarly, we calculate the Fisher information matrix (FIM) corresponding to estimating the object in the image domain, which is the same FIM used for the image-domain CRB calculations, invert it, and then pre- and post-multiply it by the appropriate matrices which generate the energy spectrum CRBs from the image-domain FIM. The image-domain CRBS are the diagonal elements of the inverse FIM matrix. The energy spectrum CRBs are the diagonal elements of the inverse FIM after pre- and post-multiplying the inverse FIM by the appropriate matrices.

The plot on the left are the energy spectrum SNRs as a function of normalized spatial frequency magnitude. Each point on the plot is the average of all the SNR values for a given spatial frequency magnitude. It can be seen that the SNRs stay above one almost everywhere, on average, for a given spatial frequency magnitude; however, there is a significant amount of fluctuation in the SNR values that make up the average SNR at each spatial frequency magnitude. The figure in the middle is the 2-D PCID energy spectrum sample variance map divided by the CRB energy spectrum map. To more easily see the ratio values that are on the order of one, the gray scales in the figure (and all the corresponding figures in the following slides) range between 0 and 4. Notice that the ratios are near one in an approximately circular region centered on zero spatial frequency. From the plot in the left-most figure, it can be seen that this is the region where the SNRs are the highest. At the highest-spatial frequencies, the ratios start increasing well beyond one, which is where the SNRs are the lowest.

As on the previous slide, the ratio of the PCID energy spectrum sample variances to the energy spectrum CRBs for each spatial frequency are plotted in the right-most figure, where the horizontal axis is SNR on a log scale, and the vertical axis is normalized PCID sample variance on a log scale. Notice that this figure shows the shape we were hoping for; that is, the PCID/CRB ratios are close to one for high SNRs, and become large for small SNRs. The transition between the two regions occurs around an SNR of 1 to 2.

We repeat the image-domain bias^2/var ratio on this screen to keep it in view. We don't calculate the bias^2/var of the energy spectrum estimates, because it is known that energy spectrum estimates are inherently biased due to measurement noise that is zero mean. When this bias is known, it can be subtracted out prior to estimating the energy spectrum. For speckle imaging, this bias is known exactly. For blind deconvolution, it isn't, so we can't subtract it out. The variances remain the same, unaffected by the biases, so that isn't an issue.

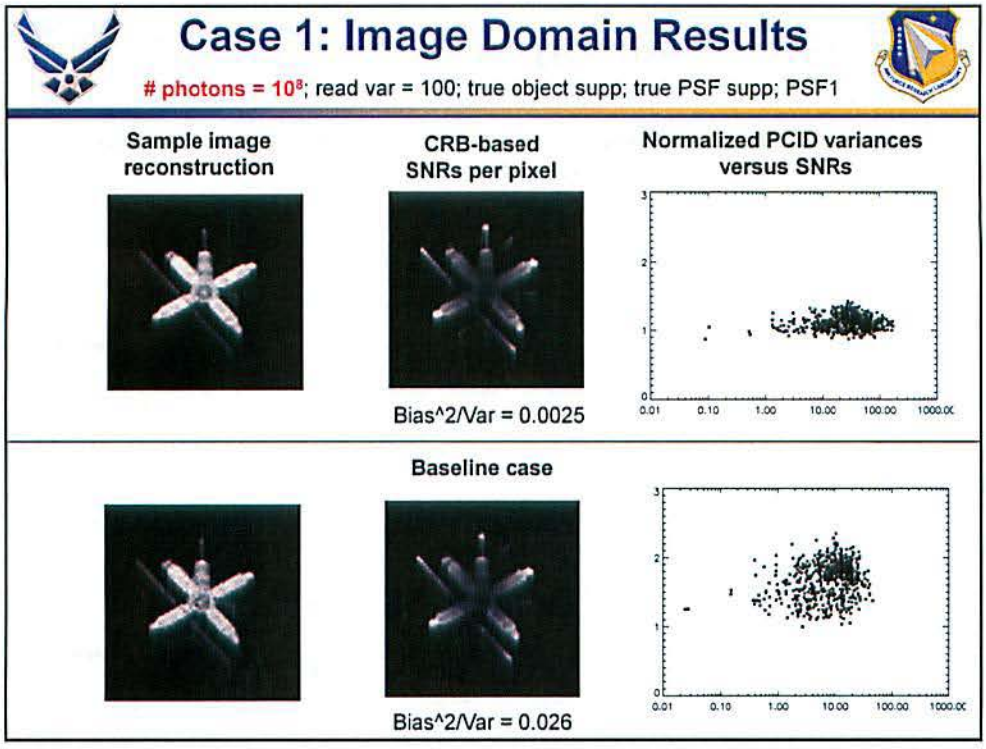

In all the remaining slides prior to the conclusion slide, the baseline case results are shown on the bottom half of the page, while the results under investigation are shown on the top half. We vary the reconstruction parameters one by one and see what their impact is.

This slides shows the image-domain results for 10^8 photons, as compared to the 10^7 photons in the baseline case. Notice that the image reconstruction is clearer, and the PCID sample variance/CRB ratios are much closer to one. Furthermore, the average bias^2/var ratio is a order of magnitude lower than for the 10^7, as is expected because there is much less chance of being trapped in local minima in the PCID cost function minimization.

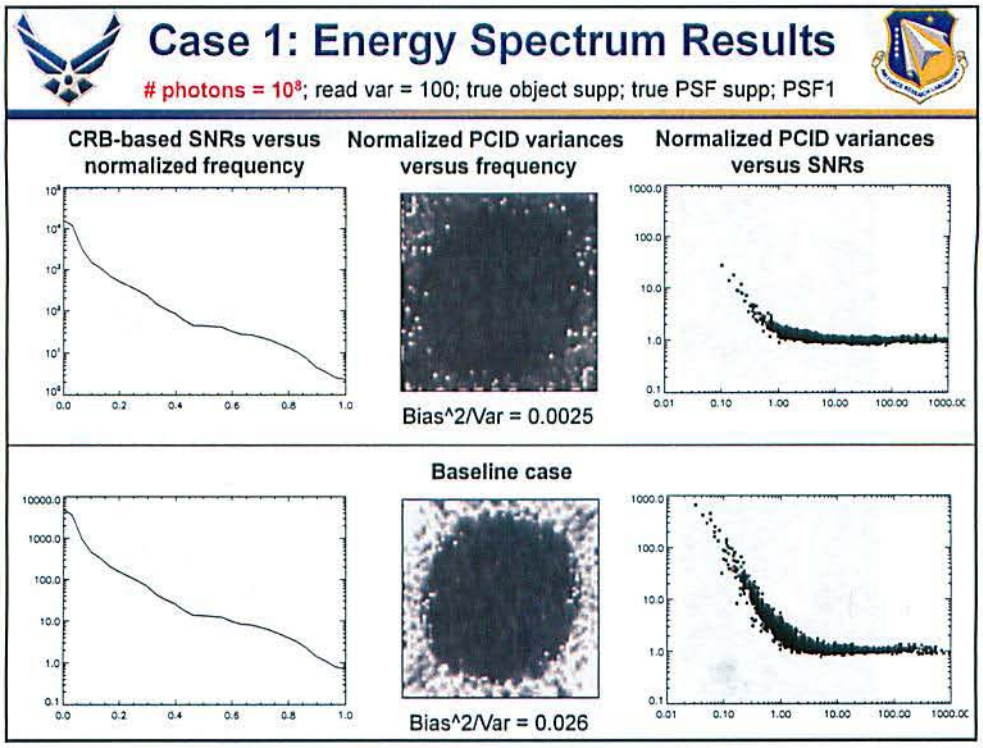

Here the energy spectrum results are shown for 10^8 photons. Notice that the energy spectrum PCID sample variance/CRB ratios are much closer to one. What is interesting is that the plot of the ratios as a function of SNR is essentially the same shape as the baseline case, just more heavily weighted to higher SNRs because of the larger number of photons.

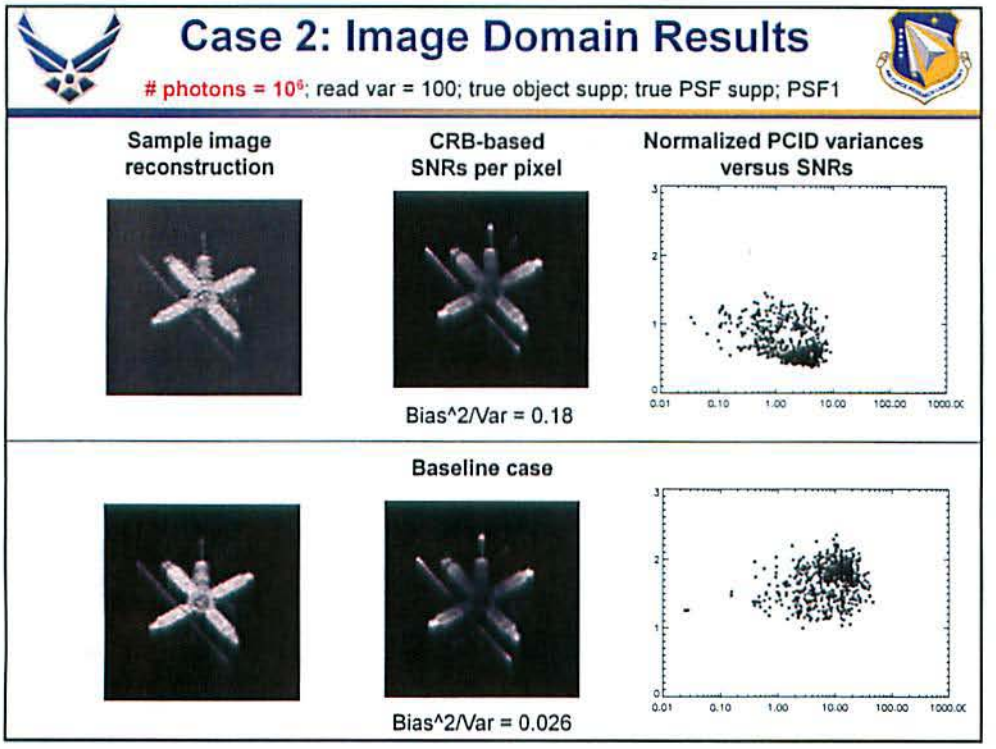

This is the 10^6 case. Notice that the image reconstruction is much noisier. Notice also that the PCID sample variance/CRB ratios are noticeably less than one. Since the CRBs are lower bounds to the variances of any unbiased estimates of the image-domain intensity values, the reconstructions must be biased. In fact, they are – notice that the bias^2/var ratio is 0.18.

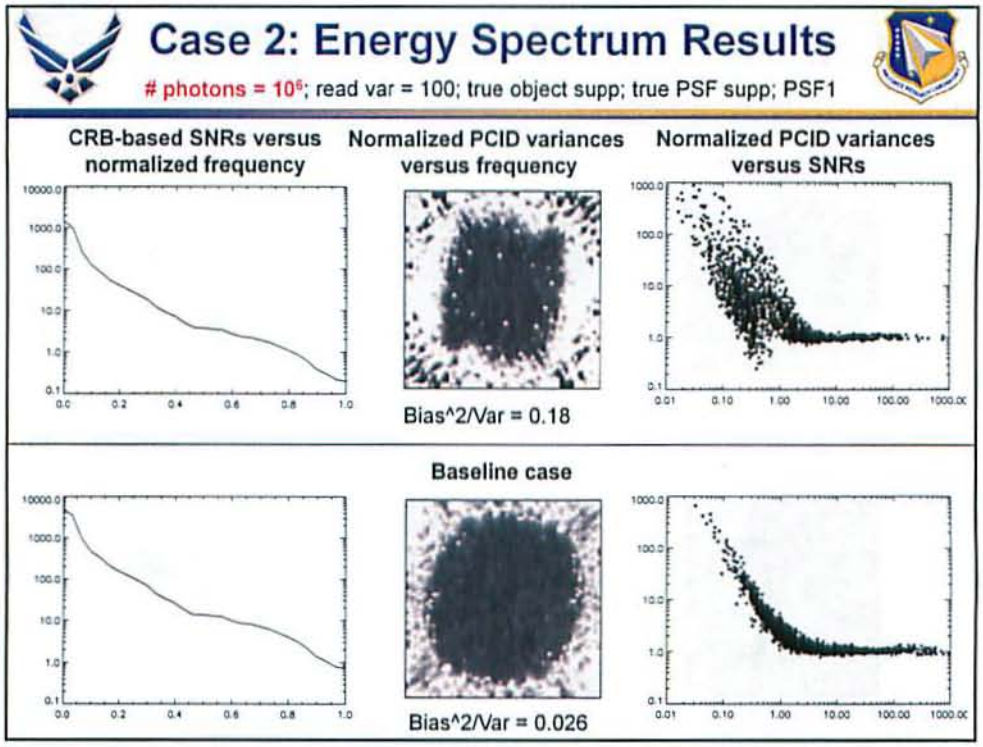

These are the energy spectrum results for 10^6 photons. Notice that the SNRs are significantly lower than the baseline case, and that there are a lot more spatial frequencies where the ratios are much greater than one. But notice that, again, the shape of the plot of the normalized PCID variances as a function of SNR is virtually identical to the corresponding plots for 10^7 and 10^8 photon levels for high SNRs. It is only in the low SNR region that the plots differ. This is an exciting result, because it indicates that including lower-SNR data points in the estimation process doesn't increase the variances of high-SNR locations.

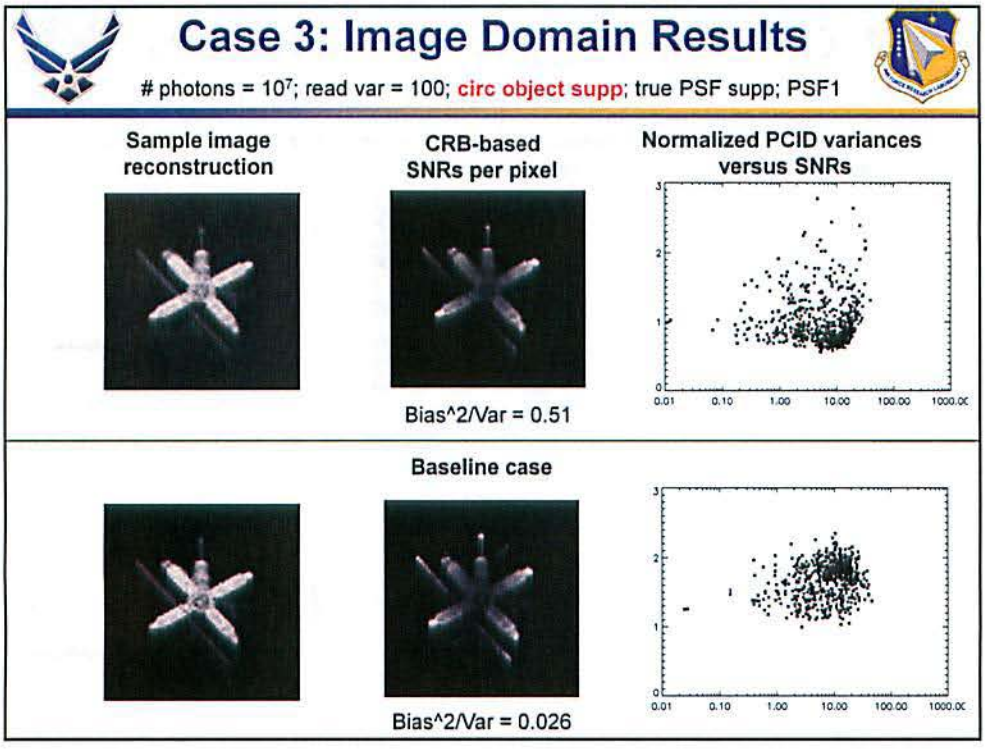

Here we go back to 10^7 photons, but use a circular object support instead of the true support. Notice that the majority of the normalized PCID variances are less than one – indicating that the PCID reconstructions must be biased. In fact they are – the bias^2/var ratio is 0.51!

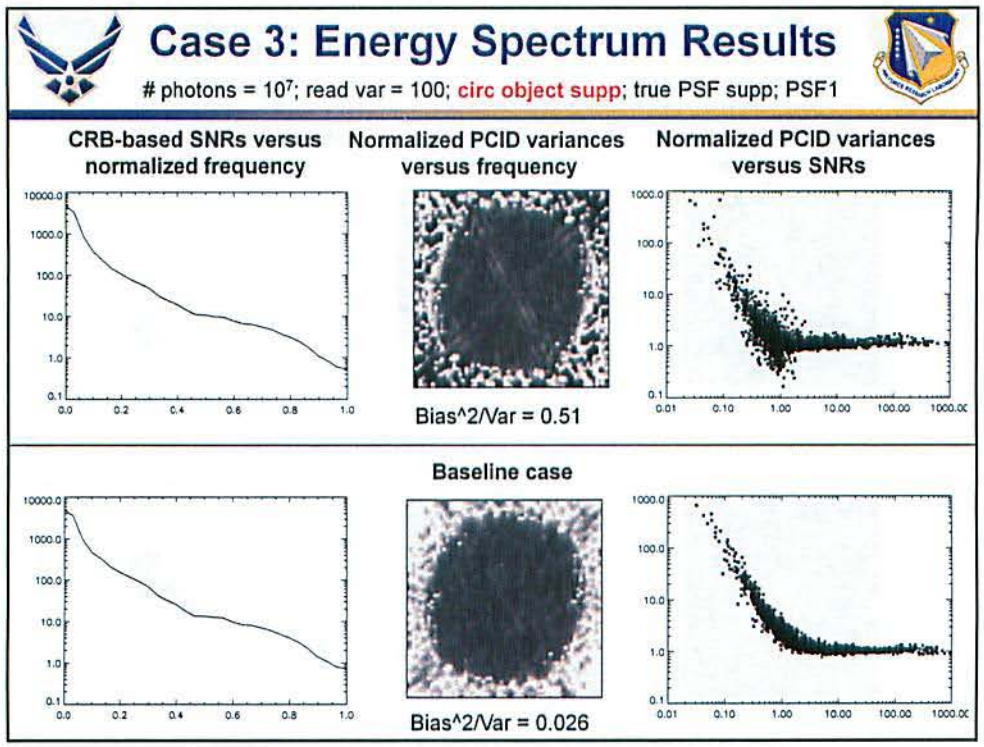

The corresponding energy spectrum results show that the PCID sample variances are still close to the unbiased CRBs for higher SNRs, so the biases must be coming from the lower SNR values.

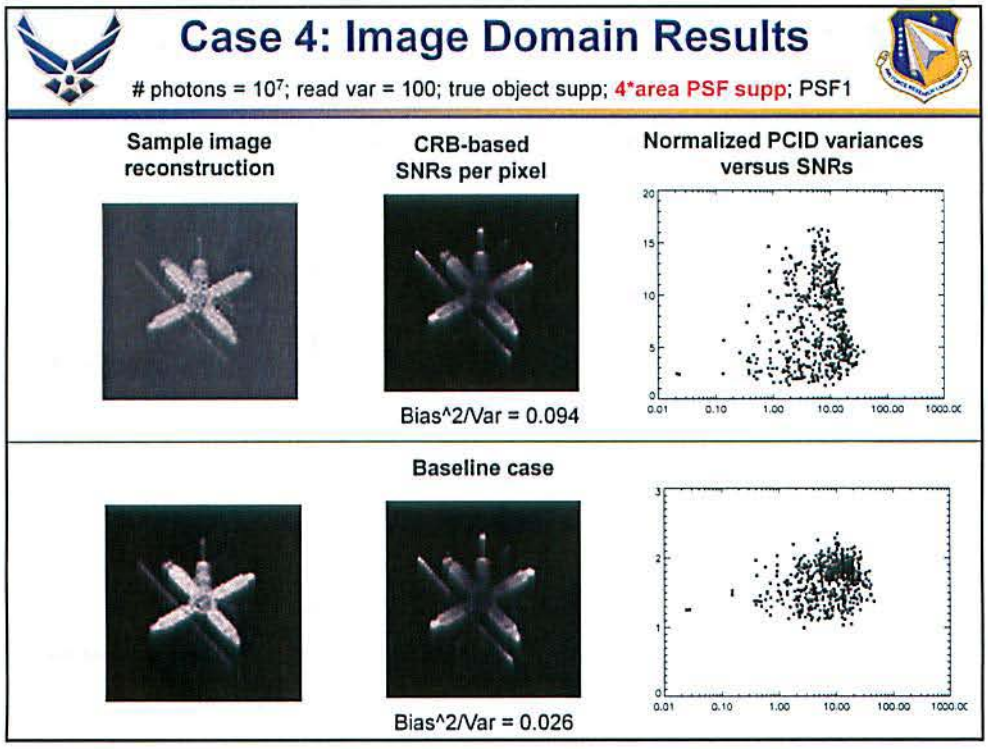

This is an interesting result. When a larger PSF support is used, the PCID reconstructions are fairly unbiased, but the normalized PCID variances are very large compared to the CRBs. The amount of noise in the sample reconstruction demonstrates the large variances.

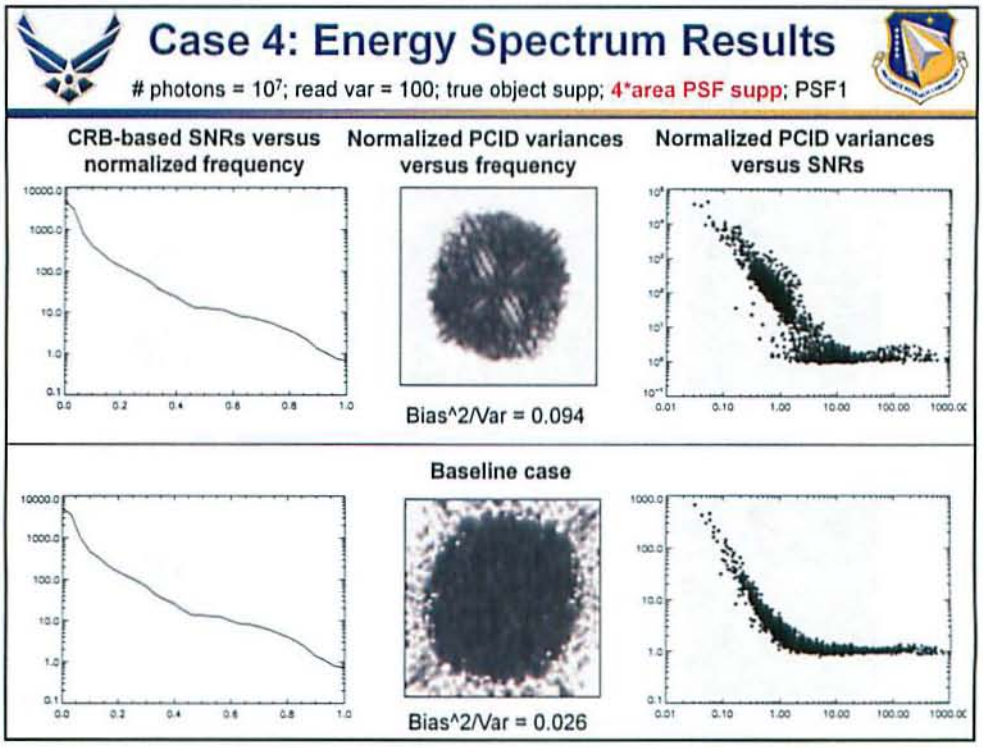

Notice that the normalized PCID variances are very large in the Fourier domain, too. Furthermore, deviation of the normalized PCID sample variances from one occurs for much higher SNRs than for any other case considered so far.

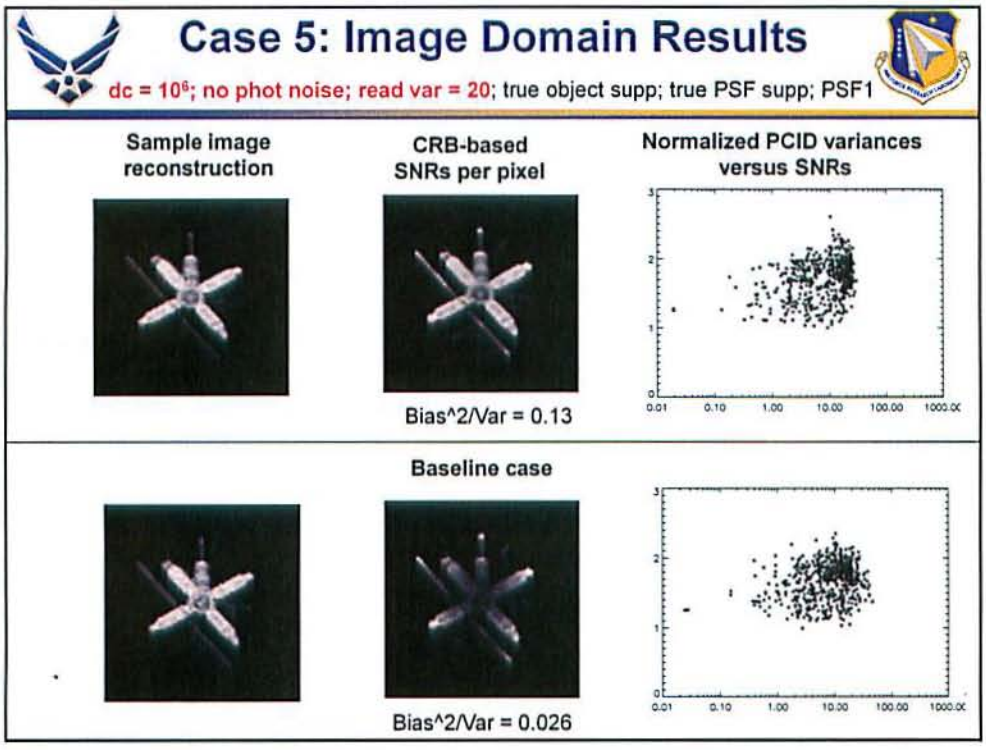

Here we have no photon noise at all; instead, we set the dc value to 10^6, and have a read noise variance of 20 per pixel. The reconstruction looks fine, and the clustering of the normalized PCID sample variances is similar to the baseline case. Notice, though that the reconstruction is relatively biased (bias^2/var = 0.13). This shows that biased reconstructions don't necessarily have correspondingly low variances. If the variances are lower than the unbiased CRBs, the reconstructions must be biased, but the converse is not necessarily true.

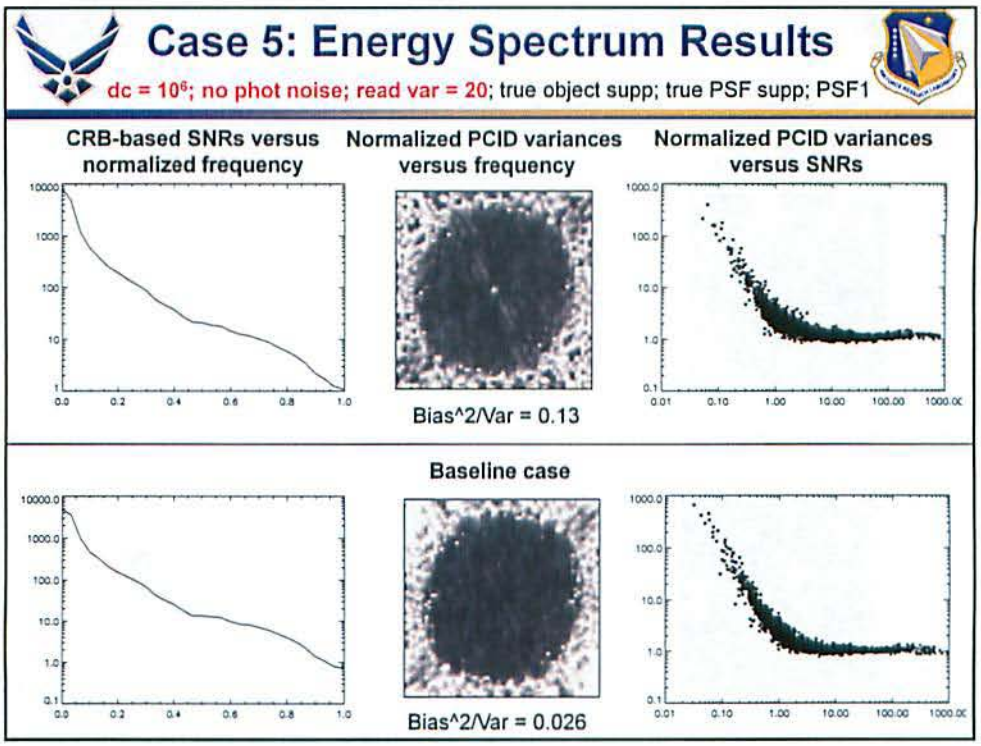

Here are the Fourier-domain results. Notice that the SNRs for the read noise case are a bit larger than for the baseline case, but that the right-most plots are approximately the same. Look next at the 2-D map of the normalized PCID variances. Notice that the variance is high right at dc, and has is higher in 'streaks' corresponding to high values of the object's energy spectrum. We have noticed this consistently with PCID reconstructions for the read-noise-only case, but don't have an explanation at this time why it occurs.

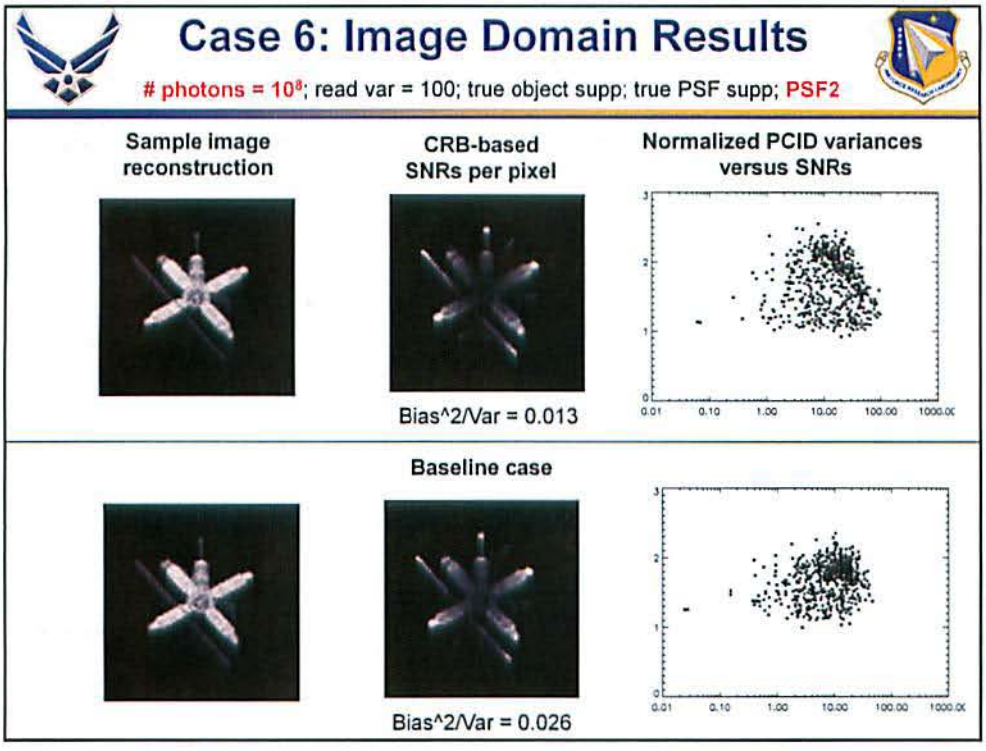

Here we replace PSF1 with PSF2. Recall that the area of PSF2 is four times as large as PSF1. This allows lower intensity portions of the underlying PSF to corrupt the images, and thus lowers the SNRs relative to PSF1. Thus, we also upped the photon level to 10^8. Notice that the results look pretty similar to the baseline case, except that the bias is half of the baseline case.

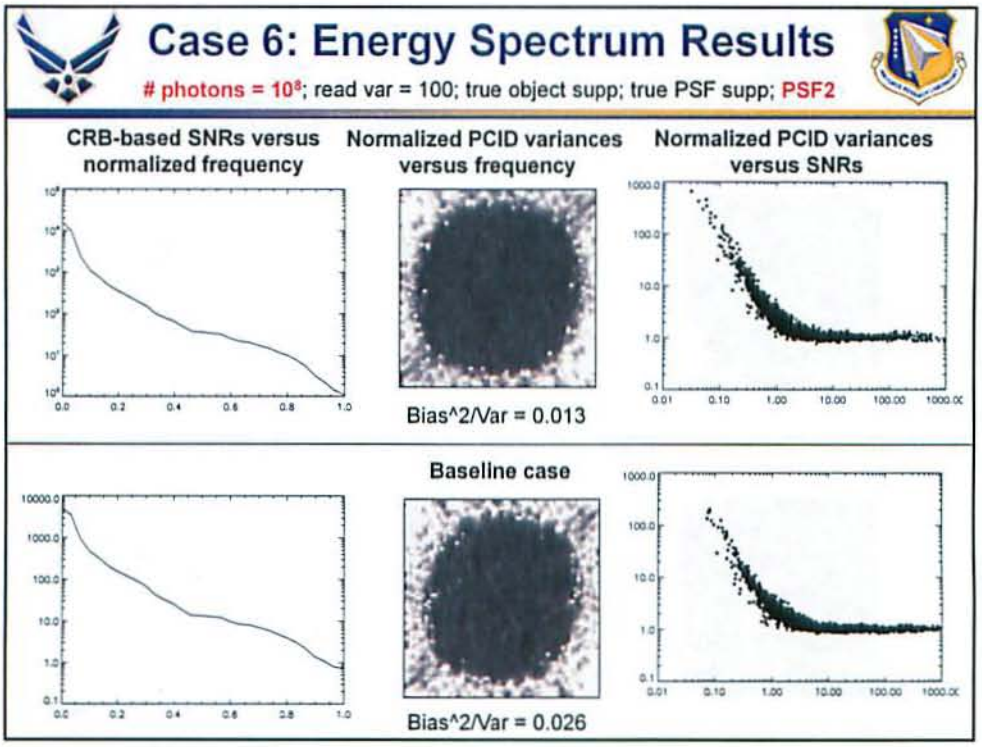

The Fourier domain results are very similar to the baseline case as well.

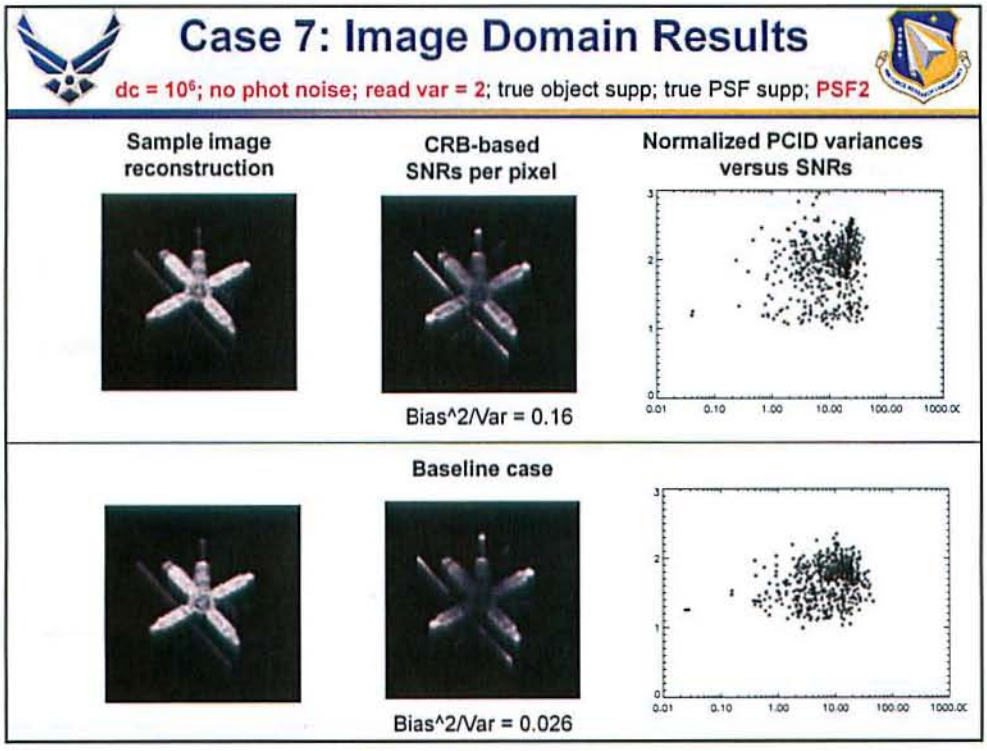

Here we use PSF2 and remove photon noise, leaving only read noise. Again, PSF2 lowers the SNRs relative to PSF1, so the read noise variance for this case was 2 instead of 20 as for PSF1. Notice that the reconstruction again is fairly biased. In addition, the sample PCID variances are larger than the baseline case.

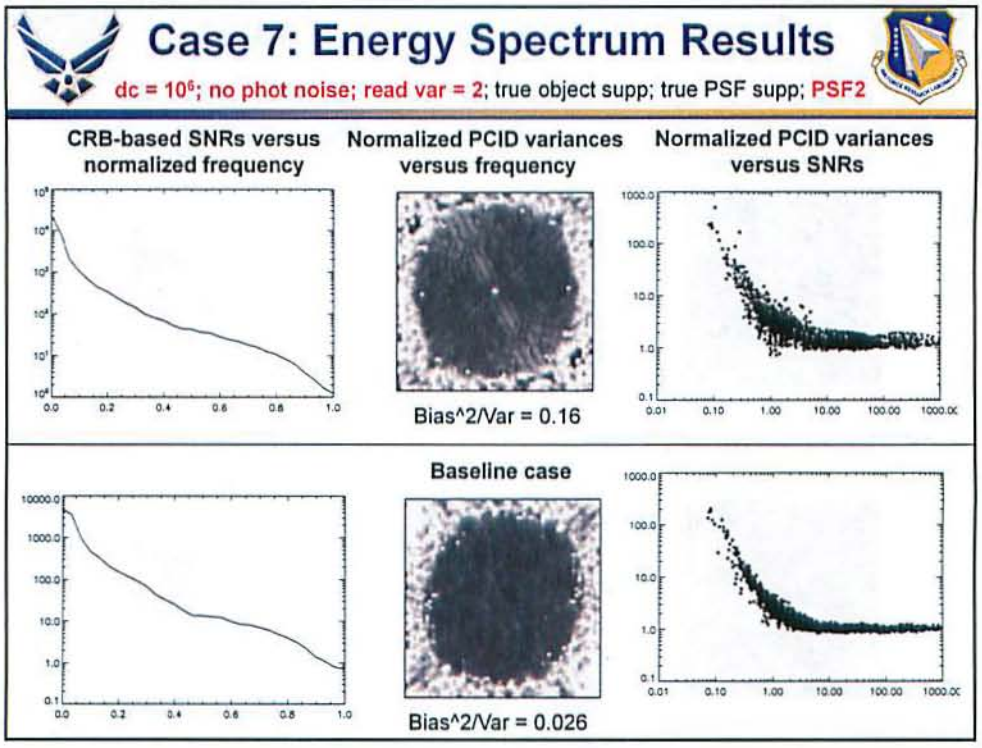

We see again the structure in the 2-D normalized PCD variance map. We also see an increased spread in the normalized PCID variances in the right-most plot, but that may be due to the accuracy for which the sample variances can be calculated.

Conclusions

- The Fourier domain seems to be a much better place to evaluate PCID performance relative to the CRBs
- When true object and PSF supports are used in the PCID algorithm, the PCID sample variances match the CRBs very well for SNRs > ~2
- When larger supports are used, PCID doesn't necessarily converge to the global minimum, and reconstructions can be biased.
- Read noise reconstructions tend to be biased, and have more structured Fourier-domain normalized variances.
- Biased reconstructions can lead to lower variances, but not always.

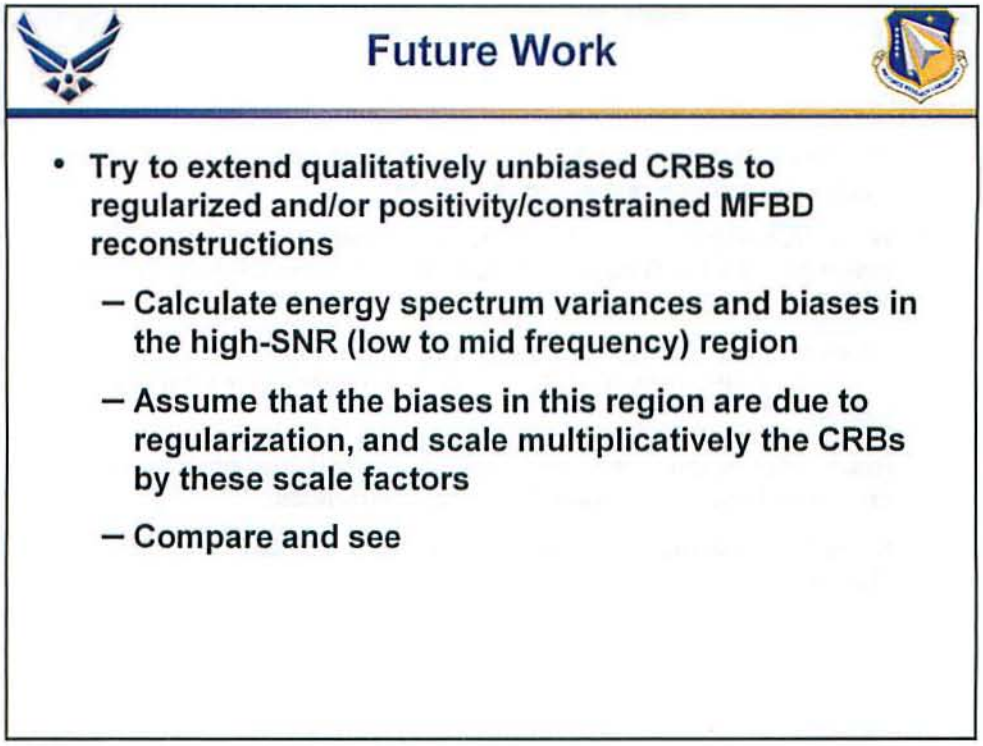

Some thoughts on how to approximate biased CRBs for positivity and regularization by unbiased CRBs and estimates of the biases

Backup Slides

Cramér-Rao Bounds

- The variances of any unbiased estimate of the pixel intensities $\hat{o}(x)$ of o(x) are no less than the CRBs (the diagonal elements of the inverse of the Fisher information matrix F):

$$\mathrm{var}\{\hat{o}(\mathbf{x})\} \geq \mathrm{diag}\left(\mathbf{F}^{-1}\right)$$

where the element of F in the k^{th} row and the j^{th} column, F_{kj}, is given by

$$\mathbf{F}_{kj} = \mathrm{E}\left\{\frac{\partial}{\partial o(\mathbf{x}_k)} \ln[\mathrm{pdf}(\mathrm{data};o)] \frac{\partial}{\partial o(\mathbf{x}_j)} \ln[\mathrm{pdf}(\mathrm{data};o)]\right\}$$

Standard text-book CRB theory

Cramér-Rao Bound Theory For Pixel-Based MFBD

- **The variances of any unbiased estimates of the pixel intensities of o(x) and $\{h_m(x)\}$ are no less than the CRBs (the diagonal elements of the inverse of the Fisher information matrix F):**

$$\mathrm{var}\left\{\left[\hat{o}(\mathbf{x}),\hat{h}_1(\mathbf{x}),\hat{h}_2(\mathbf{x}),\ldots,\hat{h}_M(\mathbf{x})\right]^T\right\} \geq \mathrm{diag}\left(\mathbf{F}^{-1}\right)$$

when F is invertible

Standard text-book CRB theory

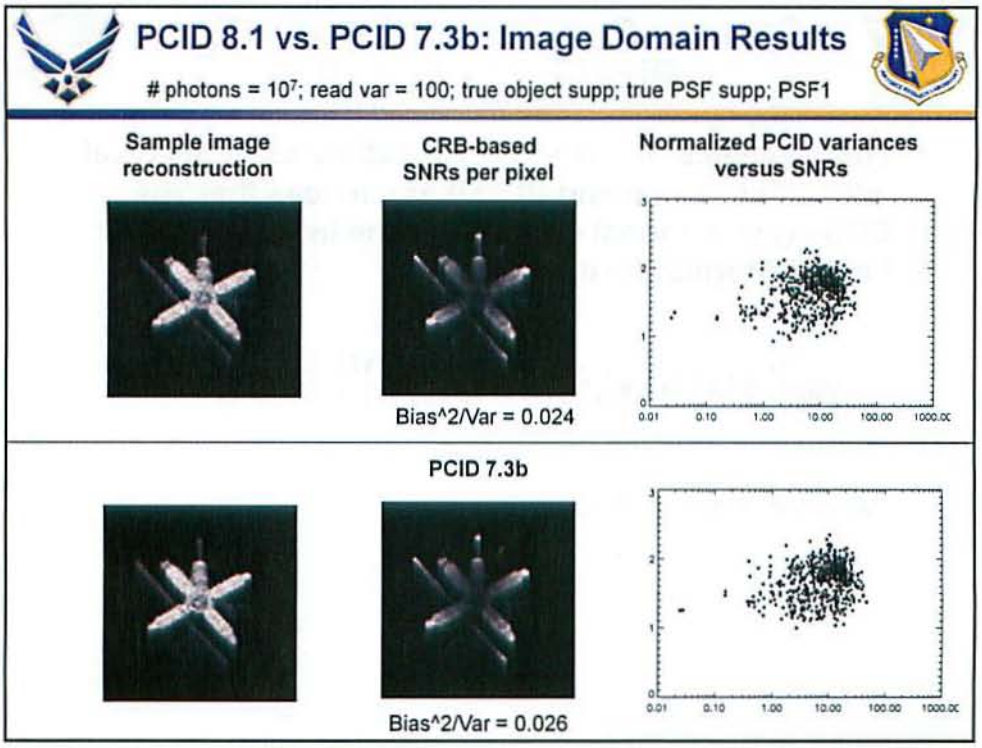

Comparison of reconstructions from an older version of PCID (7.3b) and a newer version (8.1) Notice that the results are very similar.

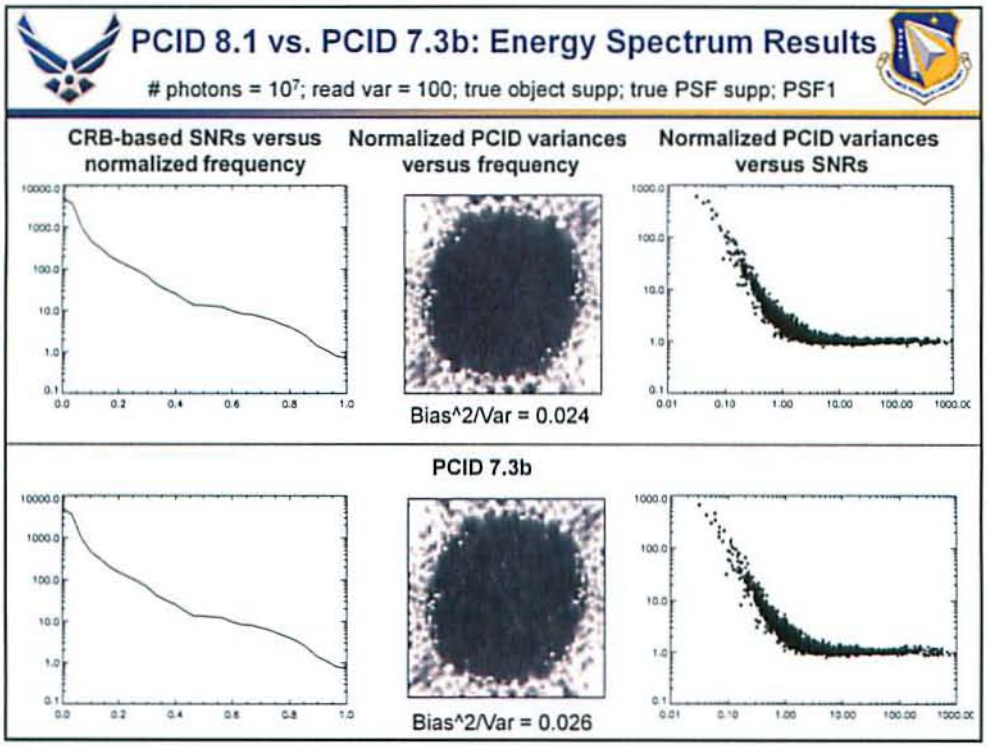

Comparison of reconstructions from an older version of PCID (7.3b) and a newer version (8.1). Notice that the results are very similar.

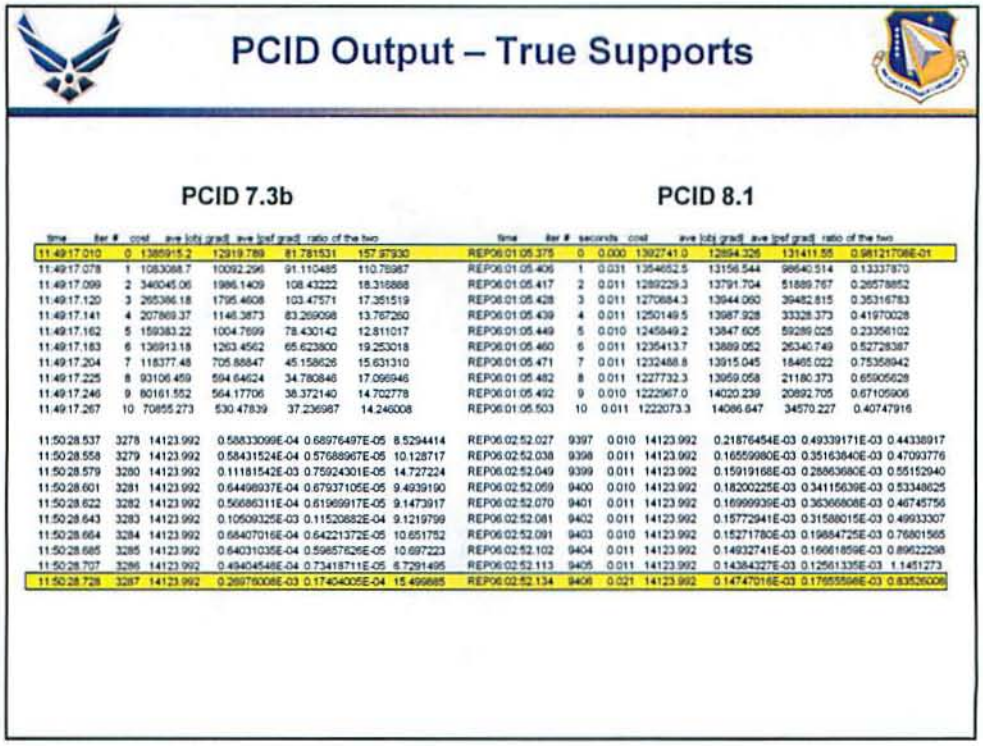

time	iter #	cost	ave |obj grad|	ave |jac grad|	ratio of the two
11:49:17.010	0	1385915.2	12919.789	81.781531	157.97930
11:49:17.078	1	1063088.7	10092.296	91.110485	110.78987
11:49:17.099	2	346045.06	1986.1409	108.43222	18.316868
11:49:17.120	3	265386.18	1795.4608	103.47571	17.351519
11:49:17.141	4	207869.37	1146.3873	83.269098	13.767260
11:49:17.162	5	159383.22	1004.7699	78.430142	12.811017
11:49:17.183	6	136913.18	1263.4562	65.623800	19.253018
11:49:17.204	7	118377.48	705.88847	45.158626	15.631310
11:49:17.225	8	93106.459	594.64624	34.780846	17.096946
11:49:17.246	9	80161.552	564.17706	38.372140	14.702778
11:49:17.267	10	70855.273	530.47839	37.236987	14.246008
11:50:28.537	3278	14123.992	0.58833099E-04	0.68976497E-05	8.5294414
11:50:28.558	3279	14123.992	0.58431524E-04	0.57688967E-05	10.128717
11:50:28.579	3280	14123.992	0.11181542E-03	0.75924301E-05	14.727224
11:50:28.601	3281	14123.992	0.64498937E-04	0.67937105E-05	9.4939190
11:50:28.622	3282	14123.992	0.56686311E-04	0.61969917E-05	9.1473917
11:50:28.643	3283	14123.992	0.10509325E-03	0.11520882E-04	9.1219799
11:50:28.664	3284	14123.992	0.68407016E-04	0.64221372E-05	10.651752
11:50:28.685	3285	14123.992	0.64031035E-04	0.59657626E-05	10.697223
11:50:28.707	3286	14123.992	0.49404548E-04	0.73418711E-05	6.7291495
11:50:28.728	3287	14123.992	0.26976008E-03	0.17404005E-04	15.499665

time	iter #	seconds	cost	ave |obj grad|	ave |jac grad|	ratio of the two
REP06.01.05.375	0	0.000	1392741.0	12894.326	131411.55	0.981217066-01
REP06.01.05.406	1	0.031	1354652.5	13156.544	98640.514	0.13337870
REP06.01.05.417	2	0.011	1289229.3	13791.704	51889.767	0.26578852
REP06.01.05.428	3	0.011	1270684.3	13944.060	39482.815	0.35316783
REP06.01.05.439	4	0.011	1250149.5	13987.928	33328.373	0.41970028
REP06.01.05.449	5	0.010	1245849.2	13847.605	59289.025	0.23356102
REP06.01.05.460	6	0.011	1235413.7	13889.052	26340.749	0.52728387
REP06.01.05.471	7	0.011	1232488.8	13915.045	18465.022	0.75358942
REP06.01.05.482	8	0.011	1227732.3	13959.058	21180.373	0.65905628
REP06.01.05.492	9	0.010	1222967.0	14020.239	20892.705	0.67105906
REP06.01.05.503	10	0.011	1222073.3	14086.647	34570.227	0.40747916
REP06.02.52.027	9397	0.010	14123.992	0.21876454E-03	0.49339171E-03	0.44338917
REP06.02.52.038	9398	0.011	14123.992	0.16559980E-03	0.35163840E-03	0.47093776
REP06.02.52.049	9399	0.011	14123.992	0.15919168E-03	0.28863680E-03	0.55152940
REP06.02.52.059	9400	0.010	14123.992	0.18200225E-03	0.34115639E-03	0.53348625
REP06.02.52.070	9401	0.011	14123.992	0.16999939E-03	0.36366808E-03	0.46745756
REP06.02.52.081	9402	0.011	14123.992	0.15772941E-03	0.31588015E-03	0.49933307
REP06.02.52.091	9403	0.010	14123.992	0.15271780E-03	0.19884725E-03	0.76801565
REP06.02.52.102	9404	0.011	14123.992	0.14932741E-03	0.16061859E-03	0.89622298
REP06.02.52.113	9405	0.011	14123.992	0.14384327E-03	0.12561335E-03	1.1451273
REP06.02.52.134	9406	0.021	14123.992	0.14747016E-03	0.17655596E-03	0.83526006

Some of the diagnostic output from one of the reconstructions used for the previous two slides.

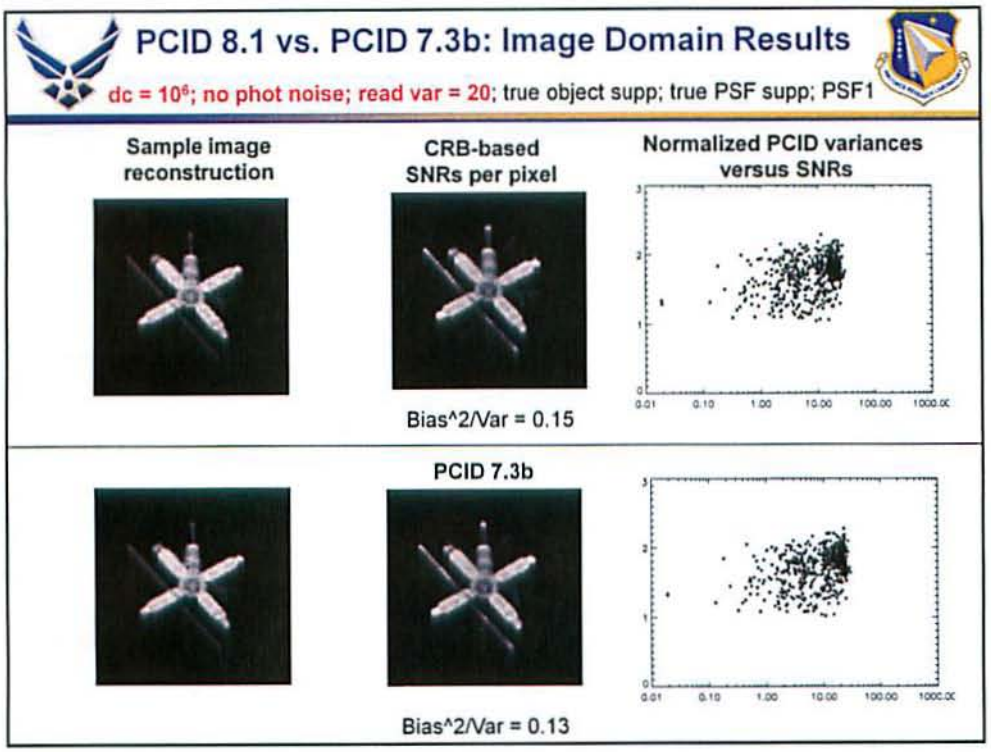

Comparison of reconstructions from an older version of PCID (7.3b) and a newer version (8.1). Notice that the results are very similar.

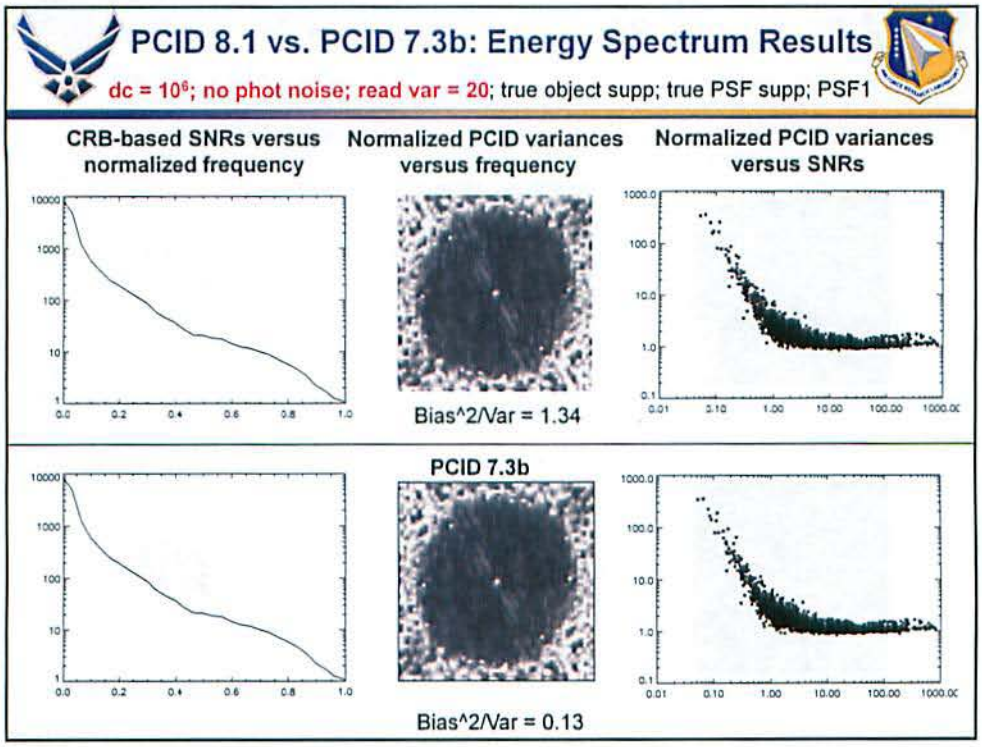

Comparison of reconstructions from an older version of PCID (7.3b) and a newer version (8.1). Notice that the results are very similar.

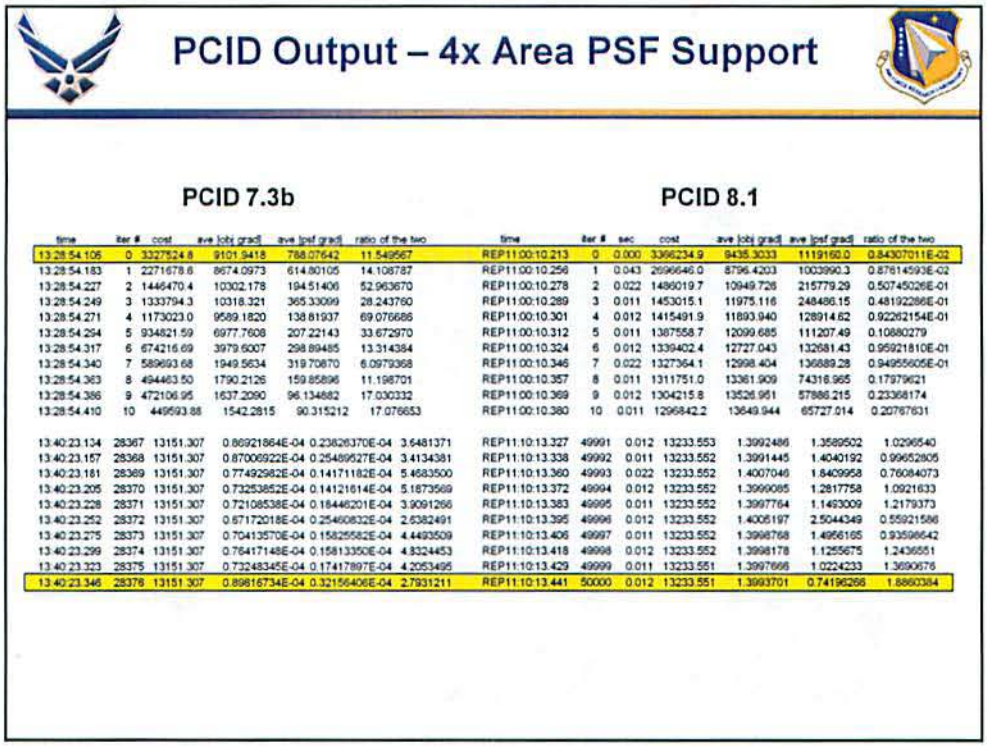

Some of the diagnostic output from one of the reconstructions used for the previous two slides.

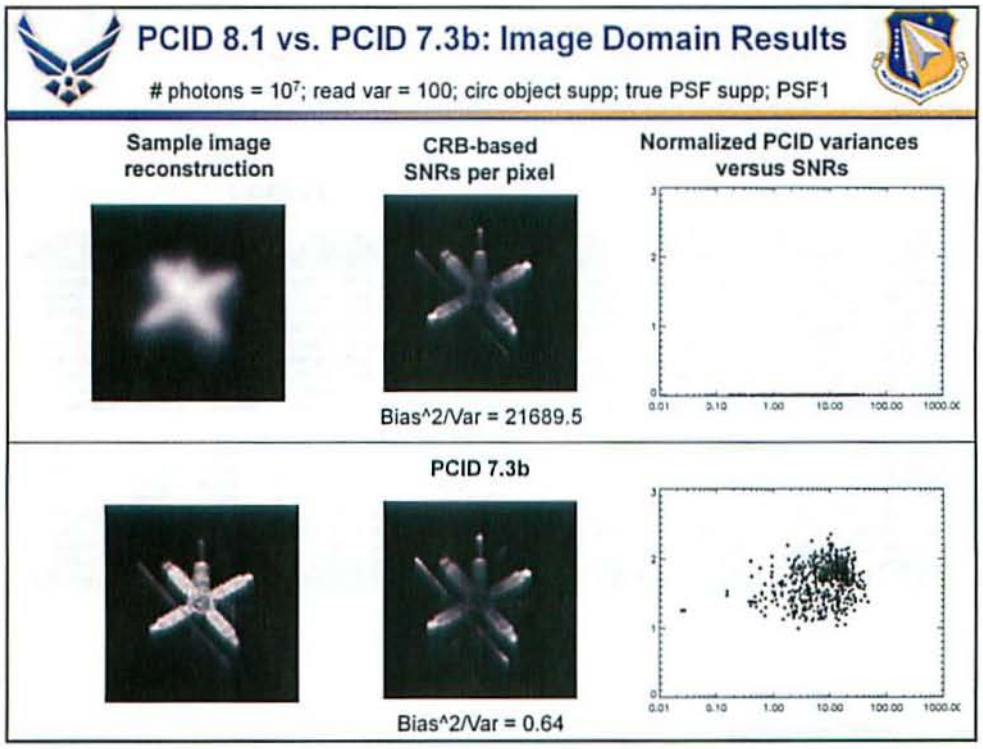

Comparison of reconstructions from an older version of PCID (7.3b) and a newer version (8.1). Notice that PCID 8.1 failed miserably to get close to the global minimum.

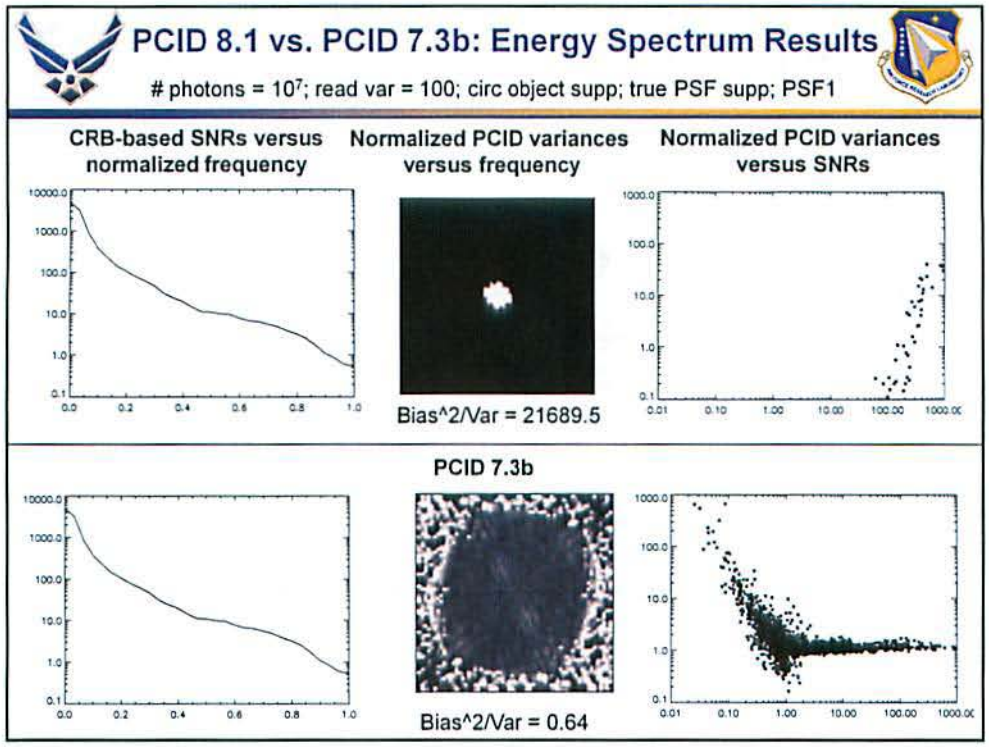

Comparison of reconstructions from an older version of PCID (7.3b) and a newer version (8.1). Notice that PCID 8.1 failed miserably to get close to the global minimum.

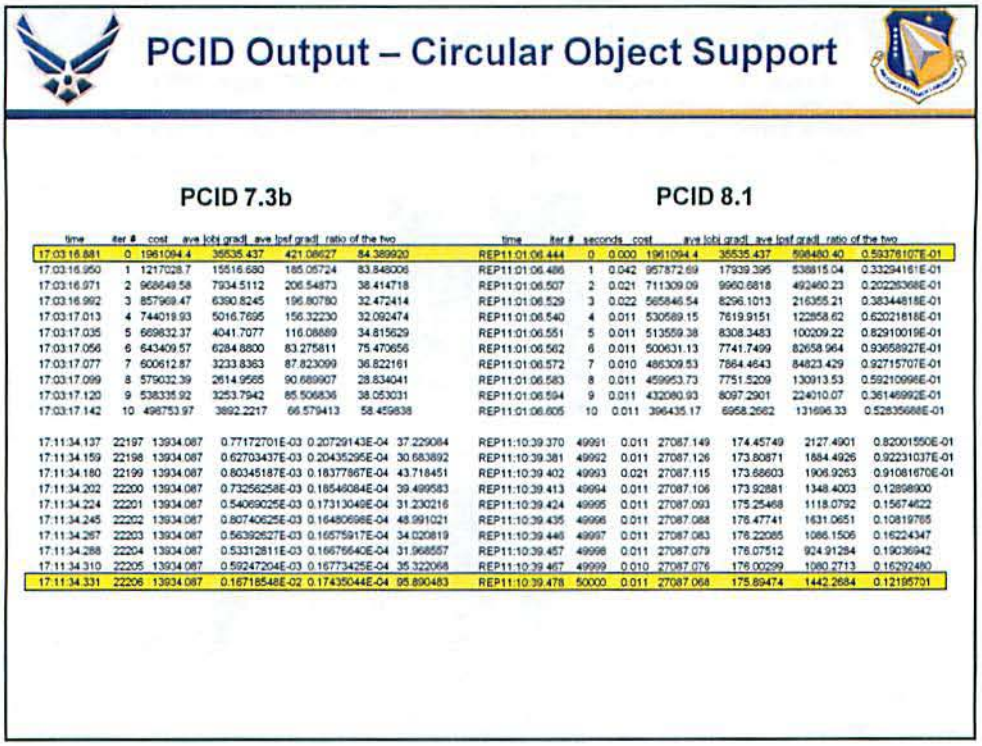

time	iter #	cost	ave lobj grad	ave lpsf grad	ratio of the two
17:03:16.881	0	1961094.4	35535.437	421.06627	84.389920
17:03:16.950	1	1217028.7	15516.680	185.05724	83.848006
17:03:16.971	2	968649.58	7934.5112	206.54873	38.414718
17:03:16.992	3	857969.47	6390.8245	196.80780	32.472414
17:03:17.013	4	744019.93	5016.7695	156.32230	32.092474
17:03:17.035	5	669832.37	4041.7077	116.08689	34.815629
17:03:17.056	6	643409.57	6284.8800	83.275811	75.470656
17:03:17.077	7	600612.87	3233.8363	87.823099	36.822161
17:03:17.099	8	579032.39	2614.9565	90.689907	28.834041
17:03:17.120	9	538335.92	3253.7942	85.506836	38.053031
17:03:17.142	10	498753.97	3892.2217	66.579413	58.459838
17:11:34.137	22197	13934.087	0.77172701E-03	0.20729143E-04	37.229084
17:11:34.159	22198	13934.087	0.62703437E-03	0.20435295E-04	30.683892
17:11:34.180	22199	13934.087	0.80345187E-03	0.18377867E-04	43.718451
17:11:34.202	22200	13934.087	0.73256258E-03	0.18546084E-04	39.499583
17:11:34.224	22201	13934.087	0.54069025E-03	0.17313049E-04	31.230216
17:11:34.245	22202	13934.087	0.80740625E-03	0.16480698E-04	48.991021
17:11:34.267	22203	13934.087	0.56392627E-03	0.16575917E-04	34.020819
17:11:34.288	22204	13934.087	0.53312811E-03	0.16676640E-04	31.968557
17:11:34.310	22205	13934.087	0.59247204E-03	0.16773425E-04	35.322068
17:11:34.331	22206	13934.087	0.16718548E-02	0.17435044E-04	95.890483

time	iter #	seconds	cost	ave lobj grad	ave lpsf grad	ratio of the two
REP11:01:06.444	0	0.000	1961094.4	35535.437	596480.40	0.59376107E-01
REP11:01:06.486	1	0.042	957872.69	17939.395	538815.04	0.33294161E-01
REP11:01:06.507	2	0.021	711309.09	9960.6818	492460.23	0.20228368E-01
REP11:01:06.529	3	0.022	565846.54	8296.1013	216355.21	0.38344818E-01
REP11:01:06.540	4	0.011	530589.15	7619.9151	122858.62	0.62021818E-01
REP11:01:06.551	5	0.011	513559.38	8308.3483	100209.22	0.82910019E-01
REP11:01:06.562	6	0.011	500631.13	7741.7499	82658.964	0.93658927E-01
REP11:01:06.572	7	0.010	486309.53	7864.4643	84823.429	0.92715707E-01
REP11:01:06.583	8	0.011	459953.73	7751.5209	130913.53	0.59210996E-01
REP11:01:06.594	9	0.011	432080.93	8097.2901	224010.07	0.36146992E-01
REP11:01:06.605	10	0.011	396435.17	6958.2662	131696.33	0.52835688E-01
REP11:10:39.370	49991	0.011	27087.149	174.45749	2127.4901	0.82001550E-01
REP11:10:39.381	49992	0.011	27087.126	173.80871	1884.4926	0.92231037E-01
REP11:10:39.402	49993	0.021	27087.115	173.68603	1906.9263	0.91081670E-01
REP11:10:39.413	49994	0.011	27087.106	173.92881	1348.4003	0.12898900
REP11:10:39.424	49995	0.011	27087.093	175.25468	1118.0792	0.15674622
REP11:10:39.435	49996	0.011	27087.088	176.47741	1631.0651	0.10819765
REP11:10:39.446	49997	0.011	27087.083	176.22085	1086.1506	0.16224347
REP11:10:39.457	49998	0.011	27087.079	176.07512	924.91284	0.19036942
REP11:10:39.467	49999	0.010	27087.076	176.00299	1060.2713	0.16292480
REP11:10:39.478	50000	0.011	27087.068	175.89474	1442.2684	0.12195701

Some of the diagnostic output from one of the reconstructions used for the previous two slides.

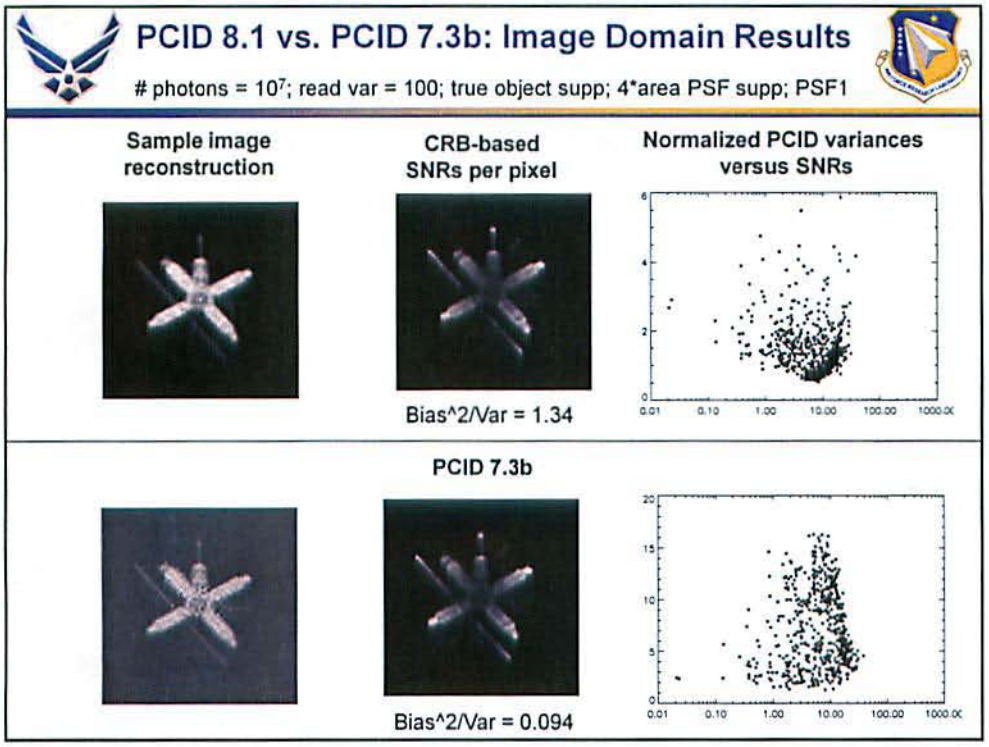

Comparison of reconstructions from an older version of PCID (7.3b) and a newer version (8.1). Notice that the PCID 7.3b reconstruction is essentially unbiased, and this shows in the noisiness of the reconstruction. The PCID 8.1 reconstruction is very biased, but has much higher visual quality.

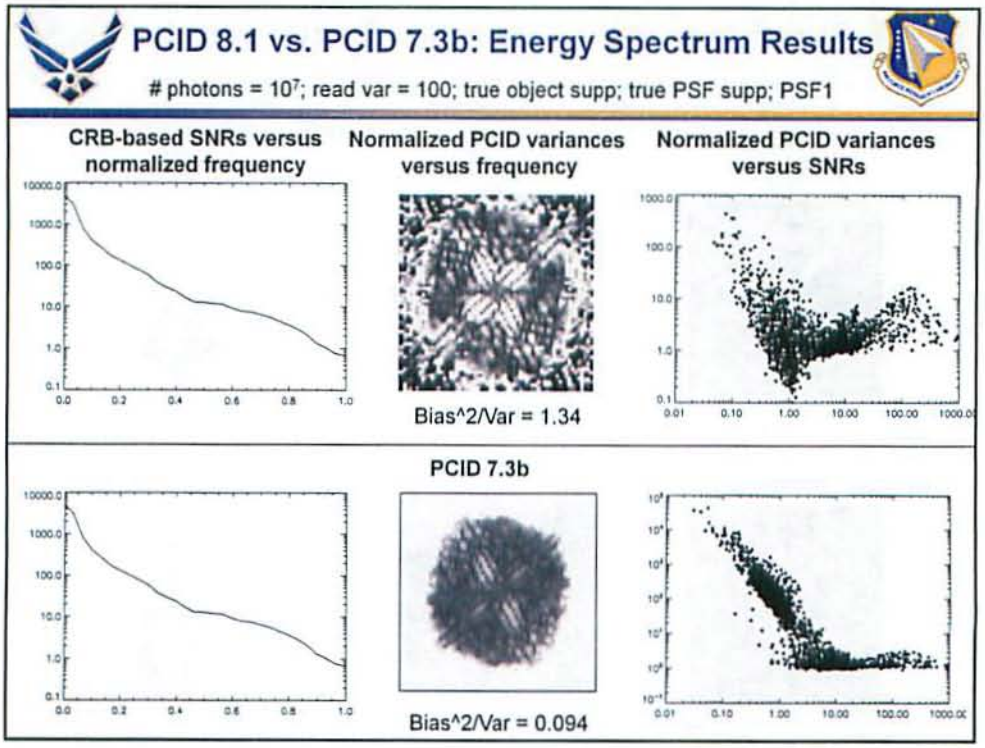

Comparison of reconstructions from an older version of PCID (7.3b) and a newer version (8.1). Notice the scale difference between the two right-most plots. The PCID 7.3b results are much noisier.

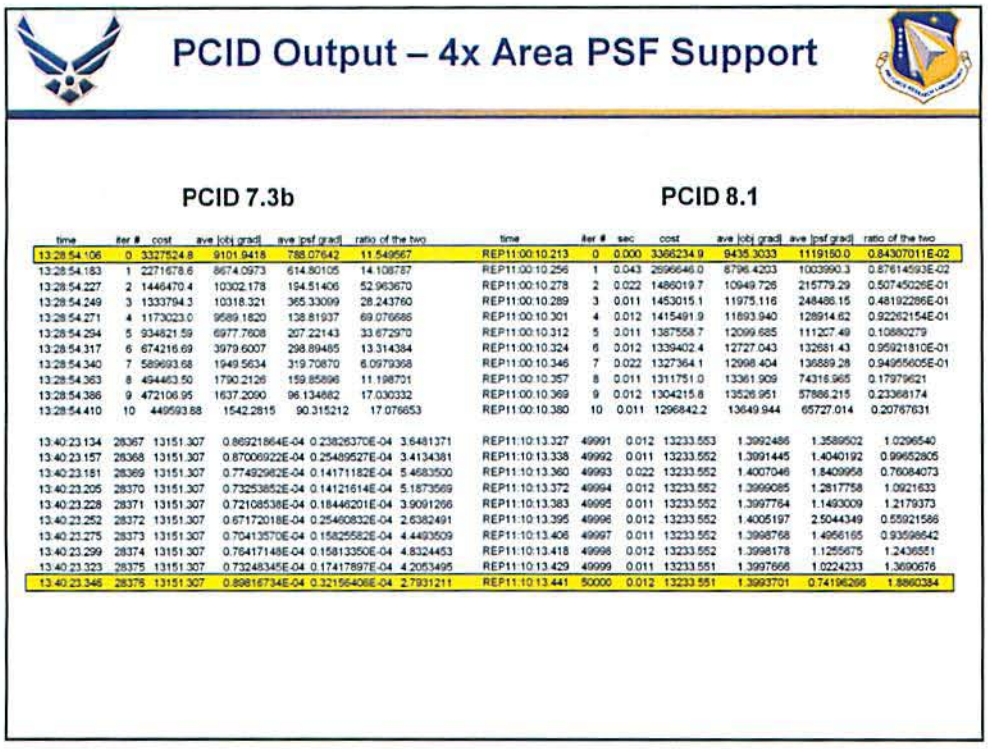

time	iter #	cost	ave [obj grad]	ave [psf grad]	ratio of the two
13:28:54.106	0	3327524.8	9101.9418	788.07642	11.549567
13:28:54.183	1	2271678.6	8674.0973	614.80105	14.108787
13:28:54.227	2	1446470.4	10302.178	194.51406	52.963670
13:28:54.249	3	1333794.3	10318.321	365.33099	28.243760
13:28:54.271	4	1173023.0	9589.1820	138.81937	69.076686
13:28:54.294	5	934821.59	6977.7608	207.22143	33.672970
13:28:54.317	6	674216.69	3979.6007	298.89485	13.314384
13:28:54.340	7	589693.68	1949.5634	319.70870	6.0979368
13:28:54.363	8	494463.50	1790.2126	159.85896	11.198701
13:28:54.386	9	472106.95	1637.2090	96.134662	17.030332
13:28:54.410	10	449593.88	1542.2815	90.315212	17.076653

time	iter #	sec	cost	ave [obj grad]	ave [psf grad]	ratio of the two
REP11:00:10.213	0	0.000	3366234.9	9435.3033	1119150.0	0.84307011E-02
REP11:00:10.256	1	0.043	2696646.0	8796.4203	1003990.3	0.87614593E-02
REP11:00:10.278	2	0.022	1486019.7	10949.726	215779.29	0.50745026E-01
REP11:00:10.289	3	0.011	1453015.1	11975.116	248486.15	0.48192286E-01
REP11:00:10.301	4	0.012	1415491.9	11893.940	128914.62	0.92262154E-01
REP11:00:10.312	5	0.011	1387558.7	12099.685	111207.49	0.10880279
REP11:00:10.324	6	0.012	1339402.4	12727.043	132681.43	0.95921810E-01
REP11:00:10.346	7	0.022	1327364.1	12998.404	136889.28	0.94956605E-01
REP11:00:10.357	8	0.011	1311751.0	13361.909	74316.965	0.17979621
REP11:00:10.369	9	0.012	1304215.8	13526.951	57886.215	0.23368174
REP11:00:10.380	10	0.011	1296842.2	13649.944	65727.014	0.20767631

time	iter #	cost	ave [obj grad]	ave [psf grad]	ratio of the two
13:40:23.134	28367	13151.307	0.86921864E-04	0.23826370E-04	3.6481371
13:40:23.157	28368	13151.307	0.87006922E-04	0.25489527E-04	3.4134381
13:40:23.181	28369	13151.307	0.77492982E-04	0.14171182E-04	5.4683500
13:40:23.205	28370	13151.307	0.73253652E-04	0.14121614E-04	5.1873569
13:40:23.228	28371	13151.307	0.72108538E-04	0.18446201E-04	3.9091266
13:40:23.252	28372	13151.307	0.67172018E-04	0.25460832E-04	2.6382491
13:40:23.275	28373	13151.307	0.70413570E-04	0.15825582E-04	4.4493509
13:40:23.299	28374	13151.307	0.76417148E-04	0.15813350E-04	4.8324453
13:40:23.323	28375	13151.307	0.73248345E-04	0.17417897E-04	4.2053495
13:40:23.346	28376	13151.307	0.89816734E-04	0.32156408E-04	2.7931211

time	iter #	sec	cost	ave [obj grad]	ave [psf grad]	ratio of the two
REP11:10:13.327	49991	0.012	13233.553	1.3992486	1.3589502	1.0296540
REP11:10:13.338	49992	0.011	13233.552	1.3991445	1.4040192	0.99652805
REP11:10:13.360	49993	0.022	13233.552	1.4007046	1.8409958	0.76084073
REP11:10:13.372	49994	0.012	13233.552	1.3999085	1.2817758	1.0921633
REP11:10:13.383	49995	0.011	13233.552	1.3997764	1.1493009	1.2179373
REP11:10:13.395	49996	0.012	13233.552	1.4005197	2.5044349	0.55921586
REP11:10:13.406	49997	0.011	13233.552	1.3998758	1.4956165	0.93596642
REP11:10:13.418	49998	0.012	13233.552	1.3998178	1.1255675	1.2436551
REP11:10:13.429	49999	0.011	13233.551	1.3997666	1.0224233	1.3690676
REP11:10:13.441	50000	0.012	13233.551	1.3993701	0.74196266	1.8860384

Some of the diagnostic output from one of the reconstructions used for the previous two slides.

DISTRIBUTION LIST

DTIC/OCP
8725 John J. Kingman Rd, Suite 0944
Ft Belvoir, VA 22060-6218 1 cy

AFRL/RVIL
Kirtland AFB, NM 87117-5776 2 cy

Charles Matson
Official Record Copy
AFRL/RDSA 1 cy